Vibrational Mean Free Paths and Thermal Conductivity Accumulation Functions for Amorphous Materials

Jason M. Larkin[1] and Alan J. H. McGaughey[1]

[1]*Department of Mechanical Engineering*
Carnegie Mellon University
Pittsburgh, PA 15213

(Dated: June 24, 2013)

Understanding thermal transport in crystalline systems requires detailed knowledge of phonons, which are the quanta of energy associated with atomic vibrations. By definition, phonons are non-localized vibrations that transport energy over distances much larger than the atomic spacing. For disordered materials (e.g., alloys, amorphous phases), with the exception of very long wavelength modes, the vibrational modes are localized and do not propagate like phonons. The Einstein model assumes that the mean free path of these localized vibrations is the average interatomic distance and that their group velocity is equal to the speed of sound. The Cahill-Pohl model assumes that the mean free path of the localized modes is equal to half of their wavelength. While these approach can be used to estimate the thermal conductivity of disordered systems, they only provide a qualitative description of the vibrations that contribute to the lattice thermal conductivity. Using lattice dynamics calculations and molecular dynamics simulations on model amorphous silicon and silica, we predict and characterize the contributions from phonons and localized vibrations to lattice thermal conductivity. The vibrational mean free paths are predicted for these two amorphous materials and the thermal conductivity accumulation function is compared with recent experimental results.

I. INTRODUCTION

Amorphous silicon (a-Si) and nanocrystalline silicon have applications in high-efficiency solar cells.(cite) Films and substrates made of a-SiO2 and a-Si have wide application in. (cite)

Thermal transport at scales comparable to phonon wave- lengths and mean free paths (MFPs) is presently a topic of considerable interest [14].[1–4]

Recently, nanostructured materials such as nanowires, superlattices, and nanocomposites with strongly reduced thermal conductivities due to phonon scattering at interfaces and boundaries have been reported and are being considered for use in thermoelectrics applications.[3–6] Recent empirical and first-principles calculations show that MFPs of phonons relevant to thermal conduc- tivity vary by more than 5 orders of magnitude in crystalline materials.[7] Traditionally, empirical expressions and simple relaxation time models have been the only means to estimate MFPs [11].[8]

The thermal conductivity of amorphous solids[9] Cahill argued that the lattice vibrations in a disordered crystal are essentially the same as those of an amorphous solid.[10]

Experimental

Broadband Techniques

Experimentally, inelastic neutron scattering has been used to measure phonon lifetimes in certain materials, but this technique is more suited for single crystal samples [13].[14] Koh et al. proposed a technique which uses a variation of modulation frequency to measure MFPs, but this technique is limited by the modulation frequency [15].[15] An x-ray diffraction and thermoreflectance technique can measure ballistic transport in some structures [14].[16]

The understanding of the accumulation function for bulk crystalline has made significant advancement experimentally[17] and theoretically.[18] However, understanding of accumulation in amorphous systems is still not well understood.[19–21] recent measurements of the accumulation function by Regner .[22]

Film Thickness Dependance

Measurements of the thermal condutivity of a-SiO_2 thin films show no significant dependance on the film thickness.[23,24] Measurements by all the refs from Galli paper, showing strong dependance on film thickness.[25–31]

a-Si

[25] find 1.8 W/m-K, similar to the SW results presented here. Yang et al find as high as 6 W/m-K.[27] Liu et al. find a film dependanc between 60 and 80 microns.[31] Claim the HWCVD method and hydrogenation creates the most ordered a-Si. zink shows no plateau at low T for a-Si thin film, indicating the scattering of long-wavelength phonon-like modes by the boundaries.[26] Show film thickness dependance up to 10 microns.[29] 4.8 W/m-K.[32]

The predictions of these theories have been difficult to test because a-Si is available only in thin-film form, making thermal conductivity and specific heat measurements difficult.

This perplexing property of glasses has been explained heuristically by assuming that phonons are scattered so strongly by structural disorder that trans- port becomes diffusive, with a frequency regime of small, constant thermal diffusivity.[75,110,114]

A. Low-frequency Scalings: w4 vs w2

The Lorentzian breadths below and above xT ;max are roughly of the forms Q2 and Q4 , respectively.[33]

In conclusion, we have reported on a new experimental determination of the elastic properties of the silica glass by means of high resolution IXS. The data give clear evidence of a Rayleigh scattering regime.[34] The acousticlike modes that persist at terahertz frequencies represent a heat conduction channel which accounts for only a fraction, although relevant, of the thermal conductivity. The failure of this approach to fully describe the conductivity data is attributed to the nondiagonal elements of the heat current operator that are not experimentally accessible.[34]

In conclusion, we have reported on a new experimental determination of the elastic properties of the silica glass by means of high resolution IXS. The data give clear evidence of a Rayleigh scattering regime. This observation repre- sents the first direct measurement of the Rayleigh law up to the BP frequency in vitreous silica, confirming the theo- retical prediction of the existence in glasses of this peculiar attenuation mechanism.[35]

B. w4

w4: as predicted for phonons scattering off point defects under the Debye approximation.

Thermal diffusivity was predicted for a percolation network which showed Rayleigh type scattering dependance in the low-frequency limit.[110]

Initial work by Zeller and Pohl[36] and later by Grabner et al.[37] demonstrated that the low-frequency, long-wavelength vibrations in glasses that dominate at low temperature can be characterized using Rayleigh type scattering, $\Lambda \propto \omega^{-4}$.

Experimental measurements of linewdiths in a-SiO2 seemed to be explained by Rayleigh scattering.[38] However, in a separate experiment on a-SiO2, a cross-over from w2, to w4, and back to w2 was observed.[39] This was confirmed by[40] and also in[41].

Theory from Schirmacher et al. predicted an w4 scaling below a system dependent onset frequency.[42,43]

A field-theoretically motivated mean-field theory self-consistent Born approximation ap- plied to this model[42,44,45] showed that the frequently observed enhancement of the vibrational DOS over the Debye one boson peak marks the crossover between wavelike and random-matrixlike states, which occurs with increasing fre- quency. In the harmonic sound attenuation this crossover re- sults in a change from a Rayleigh 4 law to a much weaker s law with s 2. This approach involves as input the statis- tics of the elastic constants, e.g., their variance and correla- tion length. Compared to the microscopical treatment this approach is much more modest, as it only qualitatively ex- plains the salient features of the vibrational spectrum of dis- ordered solids.

We show rigorously that a topologically disordered system interacting harmonically via force constants, which have a sufficiently short-ranged site-distance dependence, exhibits Rayleigh scattering in the low- frequency limit, i.e., a sound attenuation constant, which is proportional to d+1, where is the frequency and d the dimensionality.[46]

Another experiment reported Rayleigh-like scattering (and even stronger) while demonstrating that w2-like scaling can be mistaken by considering large intervals of frequency and wavelength.[47]

sound-wave scattering in a-SiO_2 shows Rayleigh type[38] numerical study of disordered lattices with varying coordination show Rayleigh type scattering.[48]

C. w2

model of a-SiO2 shows ω^{-2}[49]

the Brillouin linewidth scales like p 2 in the stable phase.[50]

w2: as predicted for phonons scattering off other phonon, where the Debye approximation is often used.

but it should be noted that published low-temperature thermal conductivity data for a-Si and a-Si:H vary with fabrication methods.[26,28,51,52]

Low temperature conductivity and specific heat measurements demonstrate that the propagating modes in a-Si and doped a-Si follow $\Lambda \propto \omega^{-2}$.[26,53] Comparison of experimental measurements by Pompe[51] and Cahill[28,52] show a plateau of thermal conductivity with temperature, which can be predicted by the the theory from FKAW which assumes a ω^{-4} scaling.[19] Zink et al. measured the thermal conductivity of e-beam evaporated amorphous silicon thin films over a wide tem- perature range and found now plateau, which is predicted from the FAB theory and an ω^{-2} scaling.[20]

Thermal conductivity of 2.0 W/m-K for $t_f = 130$ nm and 1.8 W/m-K for $t_f = 277$ nm.[26]

Fabian and Allen predict w2 dependance for model of a-Si.[54]

shows $\tau\ \omega^{-2}$ for a hard-sphere model.[55] shows w2 scaling of the inverse linewdiths from structure factor of model glasses.[56] shows w2 for long, w2.5 for tran for a model of a-SiO2.[57]

review paper on aiSO2: models and experimental data for a-SiO2 shows w2 for short wavelength, high frequency modes and scaling near w2.5 at low frequency.[58]

Using theory based on the random spatial variation of the shear modulus, a transition from w4 to w2 scaling is observed at frequencies much lower than the so-called "Boson peak" frequency.[43]

experiment from Benassi et al. show a k^2 dependance.[59]

Experimentally, for Q larger than 1 nm 1 , all glasses studied so far show $\tau \propto k^x$, with x very close to 2, see Ref. 39 for a review.

a-Si Christie et al. find a best fit of w2.5 for a model of a-Si, although adequate fits to w2 and w4 were shown.[60]

The nature of vibrations in amorphous systems in this frequency region is not yet fully understood. It is known that a force-constant-disordered crystalline lattice gives w4,[61,62] while many positionally disordered materials, including a-Si, give w2, as does a positionally disordered analytical model.[50,63]

It may therefore be positional disorder which is responsible for the reduction in the exponent from 4 to 2, although the mechanism of this reduction remains unclear. Of particular interest is the recent experimental work of Masciovecchio et al.,[39] which suggests that there may be three regimes in vitreous silica, with respectively w2 to w4 and back to w2. If this behavior is generally true, then these regions could occur at different ranges of wavevector for different materials, and this could account for different dependences being observed between different materials; the w4 dependence in lithium diborate,[47] and for the intermediate value of exponent 2.54 found for the transverse polarization by Christie et al.[60] and others.

In conclusion we have shown that in a system without any periodic order such as a monatomic liquid, one observes in- elastic excitations that can be interpreted as the noncrystal- line counterpart of Umklapp peaks.[64]

The goal of this work...

In this work, we consider two "stiff glass" amorphous systems: Structural relxation phenomena do not dominate the dynamics of the.[55]

For modeling the low frequency vibrational modes, two types of scattering mechanisms are considered: (a) phonon-phonon scattering (b) Rayleigh scattering.

BEGIN

In this work, we perform Molecular Dynamics (MD) simulations and Lattice Dynamics calculations on large models of a-SiO2 and a-Si. The results are used to understand recent experimental measurements using a broadband frequency domain thermal reflectance (FDTR) technique with varying penetration depths L_p.[22] Large MD simulations of models for a-SiO2 show (within the errors) no dependance on the system size, indicating that propagating modes do not make a significant contribution to thermal conductivity. This is confirmed by modal analysis, which demonstrates that propagating modes contribute a negligible amount to thermal conductivity. At low frequency, a quadratic scaling of the vibrational mode lifetimes is a reasonable fit to the predictions, in agreement with previous models of a-SiO2.(cite)

We predict the thermal conductivity of bulk a-Si using (to our knowledge) the largest MD simulation for a model of a-Si.(cite) Scaling of thermal conductivity with system size indicates that the low-frequency propagating modes in bulk a-Si follow a Debye-like model with a quadratic scaling of the mode lifetime with frequency. (cite) A modal analysis of a large a-Si model supports the evidence for quadratic scaling of lifetimes at low frequency, which is not definitive using the AF diffuson theory.[19,20] The propagating modes are found to contribute significantly to the thermal conductivity of a-Si an amount similar to that predicted by other models of a-Si.(cite)

The spectrum of vibrational MFPs and the accumulated thermal conductivity (cite) are predicted for a-SiO2 and a-Si. The thermal conductivity for our model of a-SiO2 accumulates within 95% of its bulk value for vibrational mean free paths (MFPs) < 10 nm. This result explains the experimental measurements of Regner et al, which show no measured dependance of the thermal conductivity on L_p,[22] and experimental measurements of the thermal conductivity of thin films which show no dependance on film thickness.(cite)

Using a simple boundary scattering model, the accumulated thermal conductivity of a-Si thin films are predicted from our model of bulk a-Si. The predicted accumulated thermal conductivity reproduces the experimentally measured penetration depth-dependent thermal conductivity qualititatively.(cite) We consider both quadratic and quartic scalings of the low-frequency vibrational lifetimes. By considering both scalings, our model of thin-film a-Si thermal conductivity accumulation can span the range of the lower(cite) and higher[27,31] experimentally measured thermal conductivity of varying thickness a-Si thin films.

The predicted contribution to thermal conductivity of non-propagating modes from our model of a-Si is in good agreement with the plateau of accumulated thermal conductivity from broadband FTDR. The quadratic scaling of low-frequency mode lifetimes does not predict the steep dependance of thermal conductivity on L_p, while the quartic scaling can qualititatively. Given the lack of experimental measurements of the low-frequency scaling of vibrational mode lifetimes,(cite) low-temperature broadband FDTR measurements can help to show which scaling, quadratic or quartic, is present in a-Si thin films with varying deposition technique. The results could answer the question of whether quartic versus quadratic scaling is responsible for the large thickness variation of the thermal conductivity of a-Si thin films.

END

II. THEORETICAL FORMULATION

A. Vibrational Thermal Conductivity

BEGIN$_A LAN$

To calculate the total vibrational thermal conductivity k_{vib} of amorphous solids, we predict the contributions from k_{ph} and k_{AF},

$$k_{vib} = k_{ph} + k_{AF}, \tag{1}$$

where k_{ph}[65–67] is the contribution from phonons or phonon-like modes and k_{AF} is the contribution from the Allen-Feldman (AF) theory of diffusons.[19] The form of Eq. has been used in several previous studies with varying assumptions. The various assumptions all lead to

predictions that k_{ph} is a significant fraction($> 20\%$) of k_{vib}.(cite)

We predict the contribution k_{ph} using a Debye-like model,

$$k_{ph} = \frac{1}{V}\int_0^{\omega_{cut}} d\omega DOS(\omega)C(\omega)D(\omega), \tag{2}$$

and the diffuson contribution k_{AF} using[19,20]

$$k_{AF} = \frac{1}{V}\sum_{\omega_i>\omega_{cut}} C_i(\omega)D_{AF,i}(\omega) \tag{3}$$

The phonon contribution k_{ph} is written as an integral because the finite simulation sizes studied in this work (and others)[19,20] limit the lowest frequency vibrational modes which can be studied. The diffuson contribution k_{AF} is written as a sum because there are enough high-frequency diffuson modes in the finite-size systems studied.[19,20] The cut-off frequency ω_{cut} identifies the transition from phonon-like to diffuson modes.[19,20,27,28,31]

Phonon-like behavior can be identified for a-Si in this work and others, both experimentally[17,22,27,31] and numerically.[19,20,68,71] Including the phonon-like contribution k_{ph} for a-Si is not qualitatively sensitive to the choice of model[19,20,31] or ω_{cut}.[19,20,27,31,70]

In this work, we identify the phonon limit by ω_{cut} in Eq. , in Section . By identifying ω_{cut} the contribution of phonon-like modes in a-Si and a-SiO_2 is quantified in Section and the thermal conductivity accumulation is predicted in Section .

B. Phonons

Eq. can be derived starting with the Kubo theory[27,34,75? ?] and taking the limit of zero phonon self-energy.[34] Eq. can also be obtained using the single-mode relaxation time approximation to solve the Boltzmann transport equation.[67] Assumed in Eq. are isotropy (valid for an amorphous material) and a single phonon polarization,(cite) making the properties a function of the mode frequency ω only. The choice of a single phonon polarization (i.e., an averaging of the transverse and longitudinal branches)(cite) does not significantly change the results predicted in this work or others.[19,20,27,28,31,34]

For a phonon gas, Eq. has mode diffusivity

$$D(\omega) = \frac{1}{3}v_g^2(\omega)\tau(\omega). \tag{4}$$

The physical picture is of propagating plane waves which travel with velocity v_g for a time τ before scattering. An equivalent physical picture in terms of a scattering length is

$$D(\omega) = \frac{1}{3}v_g(\omega)\Lambda(\omega), \tag{5}$$

where Λ is the phonon mean free path (MFP), defined as

$$\Lambda(\omega) = v_g(\omega)\tau(\omega). \tag{6}$$

Both Eq. and are valid in the propagating limit, i.e. the Ioffe-Regel limit.(cite)

In disordered system, Eqs. and are only valid in the low-frequency, long-wavelength limit.(cite) Because of this, we focus on the mode diffusivity D as the fundamental quantity. The phonon thermal diffusivity, $D_{ph}(\omega)$, is modeled using

$$D_{ph}(\omega) = B\omega^{-2} \tag{7}$$

which is a scaling predicted for Umklapp phonon-phonon scattering, (cite callaway) and

$$D_{ph}(\omega) = B\omega^{-4} \tag{8}$$

which is the scaling precited by Rayleigh scattering.[120] Both scalings Eqs. and also assume

Since we use MD simulations, which are classical and obey Maxwell-Boltzmann statistics,[72] we take the phonon and diffuson specific heat to be $C(\omega) = C(\omega_i) = \frac{k_B}{V}$ in the harmonic limit, where V is the system volume. This harmonic approximation has been shown to be valid for a-Si modeled using the Stillinger-Weber potential at the temperatures of interest here.(cite) Taking the classical limit for the specific heat allows for a direct comparison between the MD- and lattice dynamics-based methods.

While the classic limit for the mode specific heat is an over-prediction for the high frequency modes in a-Si, the non-propagating contribution predicted by broadband FTDR matches the prediction from the AF diffuson theory. Adjusting the specific heats to inclue quantum statstical effects...

We can thus focus on the less understood low-frequency propagating contribution.

Because we use molecular dynamics (MD) simulations, we

In general, the thermal conductivity k_{ph} and group velocity v_g depend on the spatial direction $\mathbf{n}$. Since the amorphous materials studied in this work are isotropic, k_{ph} and v_g are scalar quantities indepdent of the direction $\mathbf{n}$.

Under the Debye approximation, which assumes isotropic and linear dispersion (i.e., $v_g = v_s$), the denisty of states, $DOS(\omega)$, is

$$DOS(\omega) = \frac{3\pi\omega^2}{2v_{s,DOS}^3}, \tag{9}$$

where v_s is an appropriate sound speed (see Section).(cite)

The form for $D(\omega)$ (Eq.) and the $DOS(\omega)$ (Eq.) cause a cancellation of ω dependance in Eq. and ensures the thermal conductivity (Eq.) is finite. The form for $D(\omega)$ (Eq.) causes the thermal conductivity (Eq.) to diverge in the low-frequency limit as the system size is increased as $L^{1/4}$.(cite)

C. Diffusons

For disordered systems, the vibrational modes are no longer pure plane-waves (i.e., phonon modes), except in the low-frequency (long-wavelength) limit.(cite) When applied in the classical limit, the Allen-Feldman (AF) theory computes the contribution of diffusive, non-propagating modes (i.e., diffusons) to thermal conductivity[75]

$$D_{AF,i} = \frac{\pi V^2}{\hbar^2 \omega_i^2} \sum_{j \neq i} |\langle i|J_{x,y,z}|j\rangle|^2 \delta(\omega_i - \omega_j) \qquad (10)$$

where $D_{AF,i}$ is the mode diffusivity and ω_i is the frequency of the ith diffuson. The diffusivity of diffusons can be calculated from harmonic lattice dynamics theory.[19,20,75]

D. Thermal Diffusivity and Conductivity Limits

The relative contribution of k_{ph} and k_{AF} to k_{vib} has been estimated to be approximately equal for a model of a-Si at 300 K,[68] while earlier studies find that k_{ph} is less than half.[19,20] Assuming a constant contribution k_{AF} 1 W/m-K, experimental measurements and estimates show that the contribution from k_{ph} is low as 20%,[20,28] 40%,[31] and as high as,[27] all depending on the assumed scaling of the low-frequency vibrational scattering. The themal conductivity k_{vib} has also been estimated for a-GeTe[69], where $_{ph} \approx 0$ and $k_{vib} \approx k_{AF}$, and silicon nanowires,[70] where $k_{ph} \approx k_{AF}$.

For disordered materials In the low-frequency, long-wavelength limit, the mode thermal diffusivity has the form of Eq. or .(cite) The mode diffusivities generally decrease with increasing frequency,(cite) often reaching a plateau,(cite) and then decrease exponentially to zero as the modes become localized.(cite) Diffuson thermal diffusivities, Eq. , can not, in general, be expressed as either Eq. or , as the mode group velocities, lifetimes, and/or MFPs can not be estimated independently.[19,20,75,76]

It is useful to consider a high-scatter limit for the mode diffusivity,

$$D_{HS} = \frac{1}{3} v_s a, \qquad (11)$$

where it is assumed that all vibrational modes travel with the sound speed, v_s, and scatter over a distance of the lattice constant, a. This diffusivity assumption leads to a high-scatter (HS) limit of thermal conductivity in the classical limit[77]

$$k_{HS} = \frac{k_\mathrm{B}}{V_b} b v_s a, \qquad (12)$$

where V_b is the volume of the unit cell and b is the number of atoms in the unit cell.

For amorphous systems, the spatial disorder creates strong scattering, and k_{vib} tends to be near the high-scatter limit k_{HS}.(cite) It was demonstrated by Kittel that the thermal conductivity of glasses above 20 K could be interpreted using a temperature-independent high-scatter diffusivity on the order of Eq. . Since this corresponds to a phonon model with MFP $\Lambda = a$, too small to justify use of the model, implies that the dominant modes in most glasses are diffusons and not phonons.(cite)

One way to interpret this result is to use assume $k_{vib} = k_{AF} = k_{HS}$. Amorphous Lennard-Jones argon is dominated by high-scatter modes,[78] as is a model of a-GeTe, and both their $k_{vib} \approx k_{HS}$.[69] For a-SiO_2, $k_{vib} \approx 2k_{HS}$, while it is unclear what the appropriate lattice constant a should be.(cite) For a-Si, the experimentally measurred thermal conductivity at 300 K $k_{vib} \approx (1-6)k_{HS}$,[10] indicating that there may be a large contribution from k_{ph}.

While Eqs. and are commonly used to establish a high-scatter limit for diffusivity and thermal conductivity, predictions for a-SiGe alloys demonstrated that these are not true high-scatter limits.[19] Recently, the thermal conductivity of several materials has been measured to be significantly below k_{HS}.(cite)

By using lattice dynamics calculations and molecular dynamics simulations, we predict the inputs to Eq. in Section and the thermal conductivity k_{vib} in Section . The MFPs of phonons and diffusons is predicted from Eqs. and , and the thermal conductivity accumulation is predicted in Section

END$_A LAN$

III. CALCULATION DETAILS

A. Sample Preparation

1. *Amorphous Si*

For a-Si, we use models created by the Wooten-Winer-Weaire (WWW) algorithm in Ref. 79. Sample sizes with N_a = 216, 1000, 4096, and 100,000 were provided, where N_a are the number of atoms in the disordered supercell.(cite) A large sample was created from the $N_a = 100,000$ sample by treating it as a unit cell and tiling twice in all directions to create an $N_a = 800,000$ sample with box size L nm. All a-Si structures used have a density ρ equivalent to the perfect crystal with a lattice constant of a =5.43 Å.(cite)

The Stillinger-Weber potential is used with these samples. The samples were annealed at a temperature of 1100 K for 5 ns to remove meta-stability. Amorphous materials have many different atomic (potential energy) configurations with nearly equivalent energies.[80,81] The removal of meta-stability is demonstrated by an increase in the predicted sound speeds, $v_{s,T}$ and $v_{S,L}$, after annealing (see Table).[81] This meta-stability can cause errors when predicting vibrational lifetimes using Normal Mode Decomposition (NMD, see Section).(cite)

Similar structures and results can be obtained with a-Si samples created using a melt-quench-anneal procedure,(cite) similar to that used to create a-SiO_2 samples in Section .

(footnote)In an amorhous material, there are many potential energy configurations (atomic positions) which are nearly equivalent in energy. At a sufficient temperature, the meta-stable configurations cause the equillibrium atomic positions to vary in time. This can effect on the prediction of the vibrational mode lifetimes when using the normal mode decomposition method. In the time domain, the average normal mode potential and kinetic energy must be calculated and subtracted from the normal mode energy autocorrelation function.(cite) If the average energy is not specified correctly, unphysically large or small mode lifetimes can be predicted.(cite)

(footnote) The entire procedure is performed at constnat volume. Crystalline silicon (c-Si) is first melted at a temperature of 10,000 K. The liquid is then quenched instantaneously to 300 K, and then annealed at 1100 K for 10 ns to remove meta-stability.

2. Amorphous SiO_2

The a-SiO_2 samples are used from Ref. 71 and have size N_a = 288 , 576, and 972. The atomic potentials used for a-SiO_2 are the same as in Ref. 71 except the 24-6 Lennard-Jones potential is changed to a 12-6, which has a negligible effect on the predictions presented in this paper. Larger systems of N_a = 2880, 4608, and 34562 are created by a similar melt-quench technique as that used in Ref. 71

(footnote) The entire procedure is performed at constant volume. Crystalline silicon (c-Si) is first melted at a temperature of 10,000 K. The liquid is then quenched instantaneously to 300 K, and then annealed at 1100 K for 10 ns to remove meta-stability.

B. Simulation Details

Molecular dynamics simulations are performed using the disordered a-SiO_2 and a-Si supercells described in Sections and . The MD simulations were performed using LAMMPS[82] with time steps of dt = 0.00905 , 0.0005 for a-SiO_2 and a-Si. Ten MD simulations with different initial conditions were run for 2^21 time steps and the atomic trajectories sampled ever 2^8 time steps. For the GK method, the thermal conductivity k_{GK} is predicted by window averaging the integral of the heat current autocorrelation function (HCACF).(cite) For a-SiO_2 and s-Si, a interval of the the HCACF integral can be found which is constant within the statistical noise.(cite) Large system sizes up to N_a = 34,000 and 800,000 can be used to predict k_{GK} for a-SiO_2 and a-Si (see Section). For smaller systems, the trajectories from the MD simulations used for the GK method are also used in the NMD method to predict the vibrational mode lifetimes (Section).

For the amorphous supercells studied, the only allowed wave vector is the gamma-point (i.e., $\boldsymbol{\kappa} = 0$), where $\boldsymbol{\kappa}$ is the wavevector and there are $3N_a$ polarization branches labeled by ν. Calculation of the vibrational modes at the Gamma point require the eigenvalue solution of a dynamical matrix of size $(3N_a)^2$ that scales as $[(3N_a)^2]^3$, limiting the system sizes that can be considered to N_a = 4608 and 4096 for a-SiO_2 and a-Si. This eigenvalue solution is also required to perform the NMD (see Section **??**) and AF calculations (see Section IV E). The frequencies and eignvectors were computed using harmonic lattice dynamics calculations and GULP.[83] The calculation of the AF diffuson thermal diffusivities (Eq.) is performed using GULP and a Lorentzian broadening of $5\delta\omega_{avg}$ and $14\delta\omega_{avg}$ for a-Si and a-SiO^2, where $\delta\omega_{avg}$ is the average mode frequency spacing.(cite) Varying the broadening around these values does not change the resulting thermal conductivity k_{AF} significantly (see Section).

IV. VIBRATIONAL PROPERTIES

A. Density of States

In this section, we examine the frequencies and density of states (DOS) for the vibrational modes of a-SiO_2 and a-Si described in Section and . The vibrational DOS is computed by

$$DOS(\omega) = \sum_i \delta(\omega_i - \omega), \tag{13}$$

where a unit step function is used to broaden $\delta(\omega_i - \omega)$.(cite) The DOS for a-$SiO_2$ and a-Si are plotted in Fig. using two values of broadening, $10\delta\omega_{avg}$ and $100\delta\omega_{avg}$. Because of the finite model size, the low-frequency modes are sparse and the DOS has a large variability dependent on the broadening.[20] As the system size L is increased, the lowest frequency mode will continue to decrease and the gaps in frequency will fill in.(cite) The DOS for a-Si is similar to the DOS of crystalline silicon,[70,84] particularly at low-frequency, and with pronounced features as in disordered lattices.[78,85] The DOS for a-SiO_2 is essentially constant over most of the frequency-range, except at the lowest frequencies.

While the DOS has a large amount of variability at low frequency, there is a clear scaling of $DOS \propto \omega^{-2}$ for both a-Si and a-SiO_2. The range of this scaling is larger for a-Si than a-SiO_2. By fitting the DOS from Fig. to Eq. , a sound speed is predicted at reported in Table . For both a-Si and a-SiO_2, the sound speeds predicted from the DOS are close to the transverse sound speeds predicted from the elastic constants and the structure factor. The Debel model (Eq.) predicts that the contribution from the larger longitudinal sound speed compared to the smaller transverse sound speed will scale

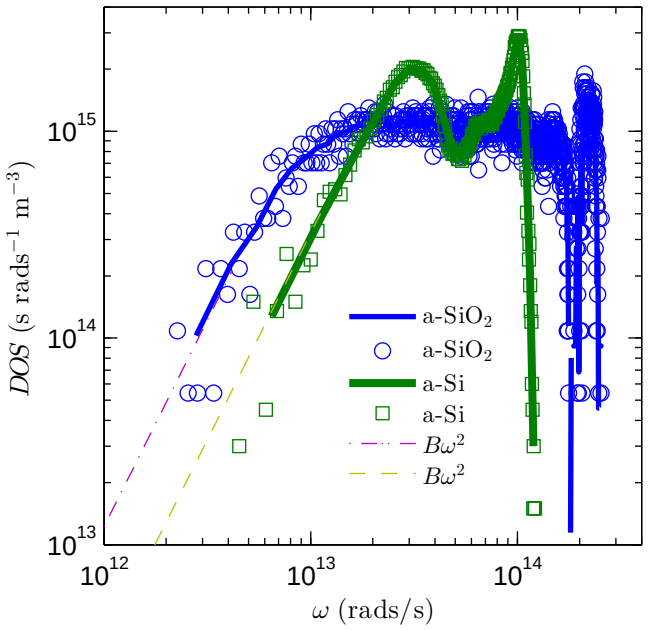

FIG. 1: Vibrational DOS predicted for our models of a-SiO2 and a-Si using Eq. (13). Both models show a scaling at low frequency $DOS(\omega) \propto \omega^{-2}$, which is predicted by the Debye approximation (Eq. (9)) using the transverse sound speeds predicted using various methods (Table I). At high frequency, the DOS of a-SiO2 shows a plateau and then a sharp feature corresponding to a gap in the vibrational spectrum due to the Si and O bonds.(cite) For a-Si, there are two sharp peaks, which show as small peaks in the preditions of the vibrational mode lifetimes (Fig. 3) and mode diffusivities (Fig. 4).

as the difference cubed. For a-Si, the contribution from longitudinal modes to the Debye DOS is nearly an order of magnitude less than the transverse modes for a given frequency interval. For a-SiO_2, the logitudinal and transverse sound speeds are closer.(cite experimental a-DOS)

The intensity for the dynamic structure factor of the TA branch was found to be 6-8 times larger than the LA branch for a model of a-SiO2.[57] A similar factor of 4-5 difference was found in the static structure factors for a mode of a-SiO2.[86] We find that the DOS for our model of a-SiO2 is also dominated by transverse modes (see Table).

The observation that the acoustic modes are located on top of a flat background for intermediate values of q has re- cently been found by G otze and Mayr as an essential result in their analytic calculation of the spectra within mode-coupling theory.[55]

The DOS predicted for jammed systems are similarly dominated by the transverse sound speed,[87] while results for disorded lattices demonstrate[78,85]

B. Group Velocity

For a disordered solid, the three acoustic group velocities (two transverse and one longitudinal) can be predicted using the elastic constants[83] or by finite differencing of the three lowest frequency branches of the dispersion relation of the supercell.[19–21,68,70,78,88] Except for this low-frequency behavior, there is not an accepted method to predict the group velocity of a vibrational mode in a disordered system, although there have been attempts.[21,68,70,77,89] In the Cahill-Pohl (CP) model, for example, the group velocity of all disordered modes is the sound speed, v_s, which is also assumed for the HS model, Eq. (**??**).[77] This assumption is not generally valid for any material.[20,21,68,70,78,89]

Experimentally determined values Freeman gives 4100 m/s for a-SiO_2[9] 3,700 5,100 from[90] for a-Si 3,800-4,800[90] Experimentally measured values of sound speed for a-Si are 4,160[91] and 4,290 m/s[92].[93] For chemical vapor depositioned a-Si thin films, the transverse sound speed is markedly increased $v_{s,T} = 4,740$ m/s.[31]

1. *From Elastic Constants and DOS*

The transverse and logitudinal sound speeds of a material can be related to the material's elastic constants, which determine the bulk (G) and shear (K) moduli.(cite) The transverse sound speed is given by(cite)

$$v_{s,T} = \frac{G}{\rho}^{1/2}, \tag{14}$$

and the longitudinal by

$$v_{s,L} = \frac{4G + 3K}{3\rho}^{1/2}. \tag{15}$$

We use the bulk and shear moduli defined in terms of the elastic constants according to the Voight convention.(cite) The sound speeds calculated from the elastic constants are reported in Table . It is clear that the DOS of our models for a-Si and a-SiO_2 are characterized by using the transverse sound speeds, rather than an averaging of the transverse and longitudinal,

$$v_s = \frac{2}{3}v_{s,L} + \frac{1}{3}v_{s,T}. \tag{16}$$

This is backed up by theoretical(cite) and experimental(cite) results.

2. *From Struture Factor*

Calculating the structure factors of the supercell Gamma modes is a method to test for their plane-wave character at a particular wave vector and polarization corresponding to the VC.[20,94] Feldman et al. used the

structure factor to predict an effective dispersion for a model of amorphous silicon, but did not predict group velocities.[20] Volz and Chen used the dynamic structure factor to predict the dispersion of crystalline SW silicon using MD simulation.[95] Has also been used to determine the dispersion relation from experimentally derived predictions.[96]

The structure factor at a wave vector $\boldsymbol{\kappa}$ is defined as[94]

$$S^{L,T}(\substack{\boldsymbol{\kappa}\\ \omega}) = \sum_{\nu} E^{L,T}(\substack{\boldsymbol{\kappa}\\ \nu}) \, \delta(\omega - \omega(\substack{\boldsymbol{\kappa}=\mathbf{0}\\ \nu})), \tag{17}$$

where the summation is over the Gamma modes, E^T refers to the transverse polarization and is defined as

$$E^{L}(\substack{\boldsymbol{\kappa}\\ \nu}) = \left| \sum_{b} \hat{\boldsymbol{\kappa}} \cdot e(\substack{\boldsymbol{\kappa}=\mathbf{0}\ b\\ \nu\ \ \alpha}) \exp\left[i\boldsymbol{\kappa} \cdot \boldsymbol{r}_0\left(\substack{l=0\\ b}\right)\right] \right|^2 \tag{18}$$

and E^L refers to the longitudinal polarization and is defined as

$$E^{T}(\substack{\boldsymbol{\kappa}\\ \nu}) = \left| \sum_{b} \hat{\boldsymbol{\kappa}} \times e(\substack{\boldsymbol{\kappa}=\mathbf{0}\ b\\ \nu\ \ \alpha}) \exp\left[i\boldsymbol{\kappa} \cdot \boldsymbol{r}_0\left(\substack{l=0\\ b}\right)\right] \right|^2 . \tag{19}$$

In Eqs. (18) and (19), the b summations are over the atoms in the disordered supercell, $\boldsymbol{r}_0\left(\substack{l=0\\ b}\right)$ refers to the equilibrium atomic position of atom b in the supercell, l labels the unit cells ($l = 0$ for the supercell), α labels the Cartesian coordinates, and $\hat{\boldsymbol{\kappa}}$ is a unit vector. Explicit disorder is included in the Gamma frequencies $\omega(\substack{\boldsymbol{\kappa}=\mathbf{0}\\ \nu})$ and the $3N_a$ components of the eigenvectors, $e(\substack{\boldsymbol{\kappa}=\mathbf{0}\ b\\ \nu\ \ \alpha})$.

The structure factors $S^{L,T}(\kappa, \omega)$ are plotted in Fig. for a-SiO_2 and a-Si (left and right panels) for wavevectors along the [100] direction of the supercells. The length scale used for the wavevectors, $\kappa = 2\pi/a[100]$, are $a =$ 4.8 and 5.43 $\mathring{A}$ for a-SiO_2 and a-Si, which are based on the atomic number densities.(cite) Frequencies $\omega_0(\kappa)$ and lifetimes $\Gamma(\kappa)$ are predicted by fitting each structure factor peak $S^{L,T}(\substack{\boldsymbol{\kappa}\\ \omega})$ to a Lorentzian function

$$S^{L,T}(\substack{\boldsymbol{\kappa}\\ \omega}) = \frac{C_0(\boldsymbol{\kappa})}{[\omega_0(\boldsymbol{\kappa}) - \omega]^2 + \Gamma^2(\boldsymbol{\kappa})}, \tag{20}$$

where $C_0(\nu)$ is a constant related to the DOS.[85] A dispersion relation is identified by plotting $\omega_0(\kappa)$ in the middle panel of Fig. , where the bars indicate the peak widths $\Gamma(\kappa)$.

For a-Si, the peaks are reasonably Lorentzian for all wavenumbers considered.[33] For a-SiO2, the peaks are Lorentzian only at the smallest wavenumbers. For large wavenumber, the structure factors peaks are much less than an order of magnitude larger than the background, and the widths are on the order of the frequency range considered in Fig. .(cite)

Sound speeds are estimated by finite differencing,

$$v_s = \frac{\delta\omega_0(\kappa)}{\delta\kappa}. \tag{21}$$

TABLE I: Estimated from the elastic constants, the pre-annealed group velocities are $v_{s,T,} = 3,670$, $v_{s,L,elas} = 7,840$ $v_{s,T,elas} = 2,541$, $v_{s,L,elas} = 4,761$ (see Section).

method	Eqs. (14), (15)	Eqs. (17), (21)	DOS Eq. (9)
a-SiO_2			
transverse	3,161	2,732	2,339
longitudinal	5,100	4,779	
a-Si			
transverse	3,886	3,699	3,615
longitudinal	8,271	8,047	

Estimates of the sound speeds are found from using finite difference of the peaks in $S_{T,L}$ are shown in Table. The values are close to those obtained from the elastic constants (see Section).

The dispersion for a-SiO_2 For intermediate κ, the longitudinal dispersion for a-SiO_2 more closely resembles the so-called "dispersion law for diffusons", where $\omega \propto q^2$.[85]

The structure factor gives the frequency spectrum needed to construct a (nonstationary) propagating state with a pure wave vector Q and pure longitudinal or transverse polarization[19]. Only low-frequency vibrations have an (approximate) wavevector in disordered systems, and there is no theorem guranteeing this.[20] you cannot assign a unique wavevector to individual modes, even for low frequency modes.[19,97,98]

Fig 4 of this work shows a dispersion extracted by locating the peaks in the structure factor. The dispersion at low frequency is also dominated by transverse sound speed.[87]

The transverse sound speed predicted by the DOS is used for both a-SiO_2 and a-Si throuhout the rest of this work.

As in other studies we find that there is a positive dispersion of the longitudinal branch initially and then there is the usual negative dis- persion at higher frequencies. The onset of this positive dispersion seems to be approximately as- sociated with the IoffeRegel crossover for trans- verse polarization.[33]

showed that when the $\tau \approx 2\pi/\omega$, the dynamical structure factor starts its collapse onto the density of states.[63] It was also demonstrated using a generic model of topologically disordered systems that both a frequency crossover of linewidth scalings, $\Gamma \propto \omega^{-2}$ and $\Gamma \propto \omega^{-2}$. Experimental measurements of a-SiO2 demonstrate such a cross-over.[39]

As the wave vector is increased, the coherence content in the dynamic structure factor tends to fade out. The spectra then merge in an effective density of vibrational states.[34]

The same positive dispersion was observe in experimental measurements of the structure factor for a-SiO2,[99] which was termed the dispersion law for diffusons.[85]

A second new observation is the presence of a softening of the acoustic modes in the frequency range where they experience strong scattering.[35]

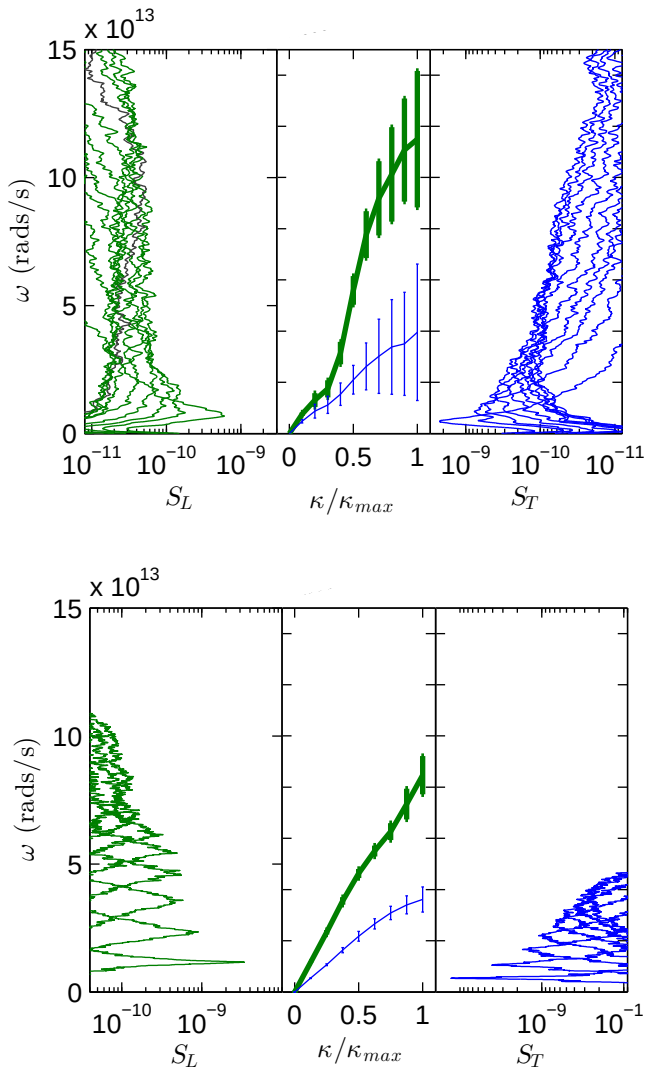

FIG. 2: Longitudinal (left panel) and transverse (right panel) structure factors (Eq. (17)) for a-SiO2 (top plot) and a-Si (bottom plot). Sound speeds are estimated by finite differencing (Eq. (21)) of the lowest frequency peaks and are reported in Table I. The dispersion for a-SiO2 is only linear for the lowest frequency, smallest wavenumbers. The dispersion for a-Si is linear over a wider range of wavenumber. Lifetimes are predicted from the widths of the structure factor peaks (Eq. (20)) and are plotted in Fig. 3.

C. Mode Lifetimes

In conclusion, we have found that the high-frequency VS in a realistic model of amorphous Si decay on picosecond time scales, and at low temperatures their lifetimes de- crease as frequency increases. This is in contrast to recent experimental claims that the modes decay on nanosecond scales and their lifetimes increase as frequency increases.[100]

The lifetimes found by this method are in good agreement with the perturbative calculations of Fabian and Allen and are on the order of 10 ps at low tem- peratures in both 216 and 4096 atom supercells.[101]

Our results indicate that all of these processes occur on a much faster time scale than the 1 ns temporal resultion of the Raman experiments, so it is not obvious that the measured relaxation rates should be identified with vibrational lifetimes.[102]

1. *From Structure Factor*

The lifetimes predicted from Eq. are plotted in Fig. for a-SiO2 and a-Si. There is a clear separation for transverse and longitudinal scalings for a-Si with $tau \propto \omega^{-2}$, and the lifetimes are above the IR limit (Eq.) for the lowest frequencies.

For a-SiO2, the separation between transverse and longitudinal is not as clear as in a-Si, and the lifetimes are significantly less than the IR limit, Eq. .

Ioffe-Regel limit[103].

2. *From Normal Mode Decomposition*

We use the MD simulation-based normal mode decomposition (NMD) method to predict the lifetimes of each vibrational mode in the disordered supercells (see Section).[73,104–106] The NMD method can predict vibrational lifetimes which are affected by the disorder in the supercell.(cite)

(footnote) In NMD, the atomic trajectories from MD simulations are first mapped onto the vibrational mode coordinate time derivative,[66]

$$\dot{q}(\overset{\boldsymbol{\kappa}=\mathbf{0}}{\nu};t) = \sum_{\alpha,b,l}^{3,n,N} \sqrt{\frac{m_b}{N}}\dot{u}_\alpha\big(\overset{l}{b};t\big)\, e^*(\overset{\boldsymbol{\kappa}=\mathbf{0}}{\nu}\ \overset{b}{\alpha}) \exp[i(\mathbf{0}\cdot\mathbf{r}_0(\overset{l}{0})]. \tag{22}$$

Here, m_b is the mass of the b_{th} atom in the unit cell, u_α is the α-component of the atomic displacement from equilibrium, $\dot{u}_\alpha$ is the α-component of the atomic velocity, and t is time. The spectral energy of each vibrational mode, $\Phi(\overset{\boldsymbol{\kappa}}{\nu};t)$, is calculated from

$$\Phi(\nu,\omega) = \lim_{\tau_0\to\infty} \frac{1}{2\tau_0}\left|\frac{1}{\sqrt{2\pi}}\int_0^{\tau_0} \dot{q}(\overset{\boldsymbol{\kappa}=\mathbf{0}}{\nu};t)\exp(-i\omega t)dt\right|^2, \tag{23}$$

The vibrational mode frequency and lifetime is predicted by fitting each mode's spectral energy $\Phi(\nu,\omega)$ (see Appendix) to a Lorentzian function

$$\Phi(\nu,\omega) = \frac{C_0(\nu)}{[\omega_0(\nu)-\omega]^2+\Gamma^2(\nu)}, \tag{24}$$

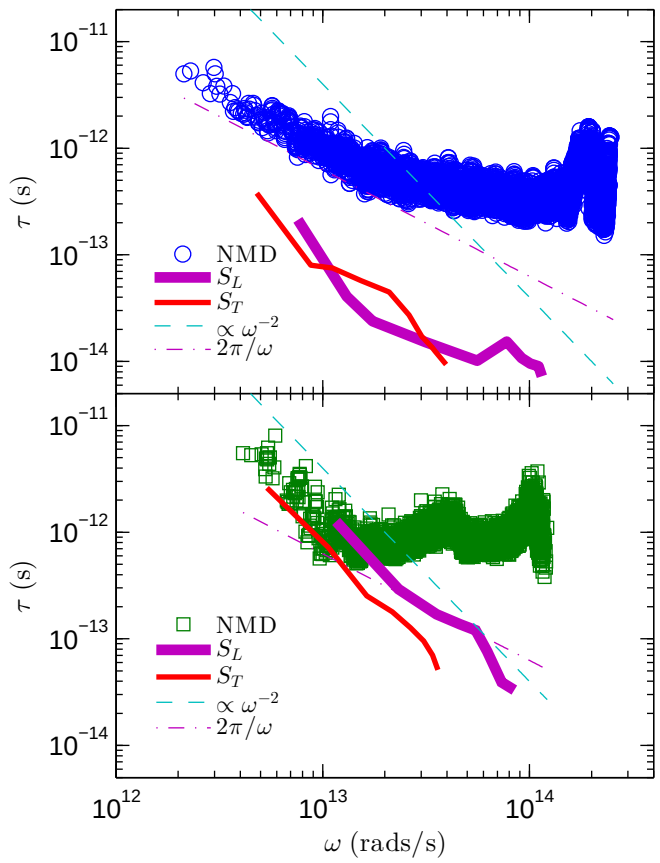

FIG. 3: vibrational mode lifetimes predicted by NMD (Eq.) and the structure factors (Eq.) for a-SiO2 (top plot) and a-Si (bottom plot). The IR limit (Eq.) is a lower limit for the mode lifetimes, while the lifetimes from the structure factors fall below this limit, partiularly for a-SiO2. The structure factor lifetimes generally follow a scaling $\tau \propto \omega^{-2}$ for both systems, while the mode lifetimes show a plateau before crossing the IR limit.

where the constant $C_0(\nu)$ is related to the average energy of each mode and the linewidth $\Gamma(\nu)$.[106] The mode lifetime is given by

$$\tau(\nu) = \frac{1}{2\Gamma(\nu)} \tag{25}$$

For a-SiO2, the mode lifetimes are generally larger than the IR limit Eq. , and follow this limit at low frequency. At high frequency the mode lifetimes are roughly constant without definite scaling. There is a peak near 2 10^{14} rads/s which corresponds to a peak in the DOS (see Fig.).

The mode lifetimes show a similar plateau at higher frequencies, particularly for a-Si, which has been reported for disordered lattices.[78]

For a-Si, a transition to a constant lifetime plateau occurs near 1 10^{14} rads/s, which corresponds to where the DOS peaks in Fig. . Similar behavior was observed for model disordered lattices.[68,78]

3. *Discussion*

It has been shown previously using MD simulation that the effect of anharmonicity on thermal conductivity is small.[107] It is not surprising that the lifetimes predicted by the structure factor (which is based on harmonic vibrational modes) agree well with lifetimes predicted by NMD, which include the effects of anharmonicity from the MD simulation.(cite)

While there is some debate as to the frequency of the cross-over from ω^{-4} to ω^{-2} from experiment.[26,35,39]

For model a-LJ, the lifetimes predicted by the static and dynamic structure factors and the NMD method are in close agreement at low temperature.[108] At low frequency for our model of a-Si, good agreement sis found between the structure factor and NMD predicted lifetimes.

The lifetimes predicted by NMD and scaled by the sound speed diverge from the AF predicted mode diffusivities when the mode lifetimes approach the IR limit, shown in Fig. . This is an indication that the modes have transitioned from propagating (where the diffusivity D and lifetime are related by $D = (1/3)v_s^2\tau$) to non-propagating where D and τ need not be related.[19,20,75,76]

For a model of a-SiO2, the lowest frequency structure factor lifetimes (inverse linewidths) are already below the IR limit.[86]

These time scales are close to those reported in Ref for similar a-Si structures. The lifetimes are also on the order of those reported for similar models of a-Si using MD-based and anharmonic lattice dynamics methods.(cite)

Fabian finds lifetimes on the order of picoseconds for a-Si and para-crystalline silicon.[100,109]

A previous study of a-Si predicted vibrational lifetimes on the order of 100 ps, about ten times the values reported here and in other studies.(cite) While the samples

For a-Si, the scaling at low frequency shows $\tau \propto \omega^{-2}$. The same scaling was found in previous studies using similar models for a-Si.(cite)

Also shown as a solid curve is the phonon gas model, where the fitted formula 1/ Q 2 i Q 2 is used for transverse i propagons, and it is assumed that transverse and longitudinal propagons have the same diffusivity. Notice that the gas- model result fits perfectly onto the higher frequency diffuson result, indicating mutual consistency of the two different transport theories in the region of overlap 10 meV 20 meV.

A numerical investigation of Bickham[102] indeed shows that a strong perturbation of the vibrational spectrum of a-Si can relax on a 100 ps time scale, compared to 10 ps for a weak perturbation. In addition to pure vibra- tional relaxation, it is also likely, as suggested by Bickham and Feldman,[101] that correspondingly large local deviations in the atomic displacements cause local structural

rearrange- ments which may relax to local metastable minima while emitting phonons.

D. Diffusivities

which generally agree with diffusivities computed according to the formula of Edwards and THoules.[20,85,111]

Thermal diffusivity has been predicted using a wave-packet method

It was shown

Garber shows that these high-frequency modes are localized in the Anderson sense, showing exponential decay of the mode eigenvector.[112]

It was shown that the diffusivity $D_{AF}(\omega) \propto DOS(\omega)$ at low frequency when the modes are spatially uncorrelated and the overlap between them is small and independent of the frequency.[87,113] This result helps to explain the plateau of diffusivity for both a-SiO2 and a-Si at higher frequencies. The features in $D_{AF,i}$ for both a-SiO2 and a-Si can be exaplined by peaks in the DOS at these frequencies.

Based on the NMD-predicted diffusivities, the modes at low frequency are dominated by transverse modes. However, given the scatter in the NMD-predicted lifetimes, there is some mixture of transver and logitudinal modes at low frequency. Treating these two branches separately is not necessary since similar results are obtained by assuming a single branch scaling $D(\omega) = B\omega^{-2}$ which is fit to coincide with the peak in diffusivity D_{AF} at ω_{cut} = 11.6 E 12 rads/s. This choice of ω_{cut} is close to that used by FAB (ω_{cut} = 9.65 E 12 rads/s),[19] and is somewhat smaller than that used by FKAW[20] and Cahill et al.[28] (ω_{cut} = 15.2 E 12 rads/s).

This choice of ω_{cut} is motivated by the AF predictions, gives a resonable fit to the NMD predictions, and also an extrapolated total thermal conductivity k_{vib} which is in reasonably good agreement with k_{GK} (Fig.).

For a-SiO2, we find the same ω_{cut} = 4.55 rad/s as used in Ref 34 and a quadratic scaling gives a reasonably good fit to the low-frequency diffusivities predicted by the AF theory (Fig.). In this work, the predicted contibution k_{ph} = 0.10 W/m-K is close to that predicted by Ref. 34. Within the errors of the predictions, the predicted k_{ph} for a-SiO2 is not significant, contributing about 5% to k_{vib}.

At low frequencies, the AF-predicted and NMD-predicted mode diffusivities scale as $D \propto \omega^{-2}$, similar to the scaling due to Umklapp scattering of phonons in a crystalline system. Rayleigh scattering due to point defects predicts $D \propto \omega^{-4}$, but is not observed in the amorphous systems studied in this work.(cite) While quartic scaling has been observed in harmonic studies of the diffusivities of modes in disordered lattics and jammed systems,[87,110,113] it has been demonstrated that the harmonic disorder in a-Si produces a scaling similar to Umklapp scattering.[19]

Both a-SiO_2 and a-Si have a region at higher frequencies where the AF-predicted mode diffusivities are relatively constant. This behavior has been reported for a number of model disordered systems such as disordered lattices[78,85,110], amorphous solids,(cite) and jammed systems.(cite) At the higest frequencies the AF-predicted diffusivities trend exponentially to zero, which is an indication that these modes are "locons", spatially localized modes which do not contribute to thermal condutivity.[94,112]

Based on the lifetimes predicted from NMD, the diffusivities D_{NMD} predicted at low frequency for a-Si follow very closely the scaling $D(\omega) \propto \omega^{-2}$ (Fig.). The mode diffusivities show much less scatter than those predicted by the AF theory D_{AF}, which is due to the finite-size system and the broadening which is required to evaluate Eq. (10).[19] By using a much larger broadening ($100\delta\omega_{avg}$) the scatter in the AF-predicted diffusivities at low frequency can be smoothed, but at the cost of decreasing the diffusivities at intermediate and high frequencies. It is possible that a frequency-dependent broadening may be necessary for a-Si, but determining this dependence is not clear nor necessary for interpreting the results in this work.

Because the AF-predicted diffusivities show a large scatter, both ω^{-2} and $\omega-4$ scalings can be considered as "fits" to the low-frequecy behavior. Both FKAW and interpretation of experimetnal results by Cahill et al. have used ω^{-4} scaling at low frequency.

Our models of a-SiO2 and a-Si also

Using the NMD-predicted lifetimes and AF-predicted diffusivities, a representative velocity can be computed,

$$v_{AF}(\omega) = \left(3\frac{D_{AF,i}(\omega)}{\tau(\omega)}\right)^{1/2}, \tag{26}$$

and is shown in the inset of Fig. . For a-Si, v_{AF} follows a decreasing trend with increasing frequency, similar to the trend for group velocities in a simple monatomic crystal.(cite)

The dependence of v_{AF} in frequency is similar to that found for simple crystalline systems, where negative dispersion typically causes a decrease of group velocity with increasing frequency (or wavevector).(cite) Negative dispersion has been predicted by many models of both a-SiO2 and a-Si,[116] as have experimental measurement of dispersion relations.(cite) The effective group velocities which have been prediced using dispersion relations near zero wavevector for large supercells of amorphous[21,68] and disordered lattices[88] would appear to be underestimates compared with the effective velocities v_{AF} predicted in this work, where v_{AF} is within a factor of three of v_s for all but the highest frequency, localized modes.(cite) Our predictions for v_{AF} also support the notion of a minimum thermal diffusivity on the order of D_{HS} for all vibrational modes except those which are localized (the so-called "locons").(cite)

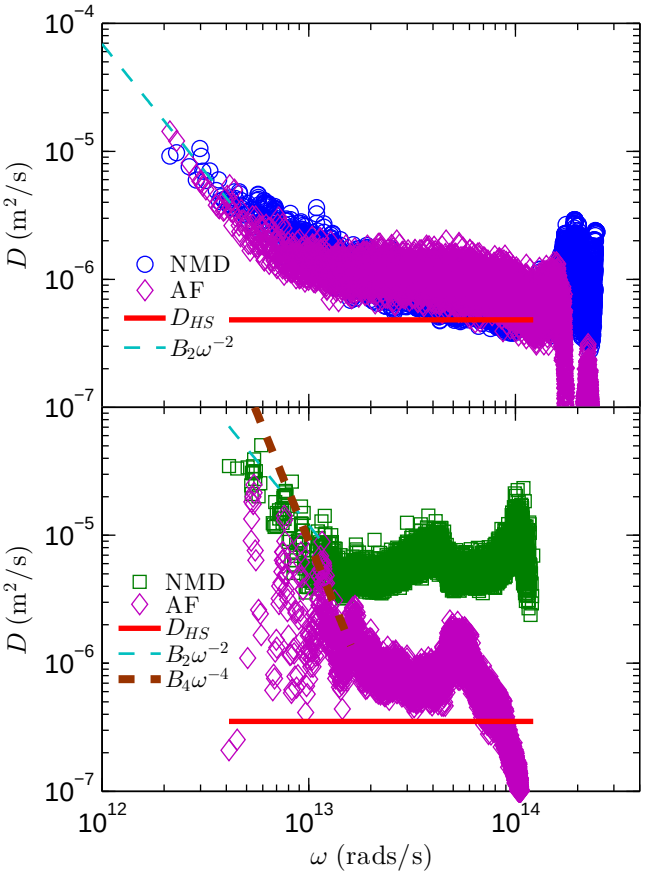

FIG. 4: vibrational mode diffusivities predicted from NMD (using Eqs. (4) and (25) with the sound speed $v_{s,DOS}$ from Table I) and AF theory (Eq. (10)). Also shown are the extrapolations Eqs. (7) and (8), which are used with Eq. (2) to predict the thermal conductivity accumulations in Fig. , and the high-scatter limit Eq. (11).

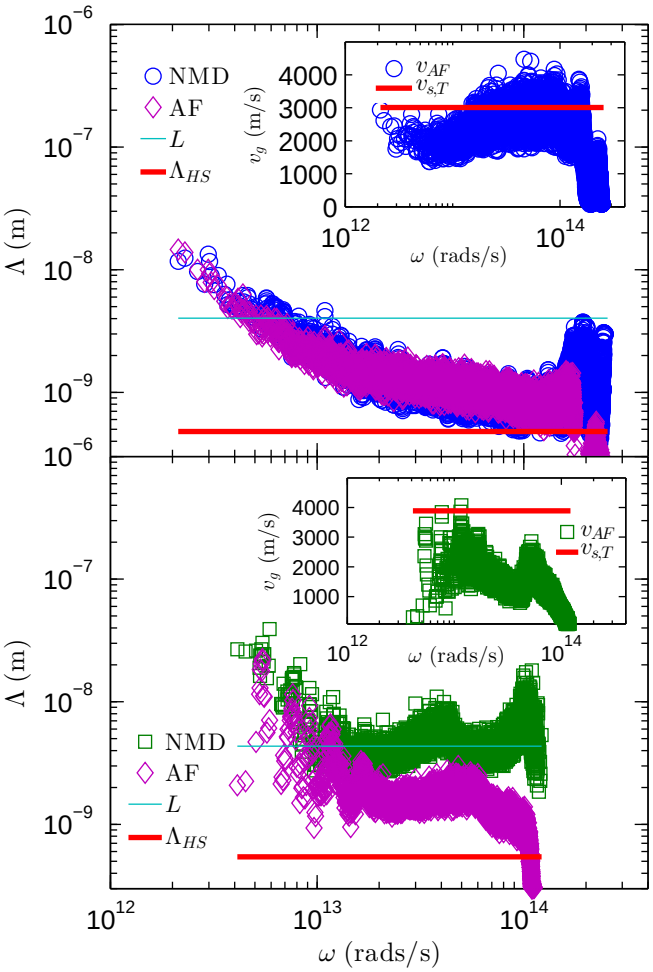

FIG. 5: vibrational MFPs predicted from NMD using Eq. (6) and the sound speed predicted in Table I and from NMD and AF using Eq. (27). Good agreement between the two methods is seen at low frequency, indicating that the modes are propagating and Eqs. (4) and (5) are valid. The majority of MFPs in the intermediate the high-frequency range lie between the simulation box size L and the bond distance a. The inset compares the representative mode velocities Eq. (26) and the sound speeds. For a-Si, v_{AF} decreases with increasing freuquency, similar to the behavior of a monatomic crystal.(cite) The MFPs and mode velocities only approach zero at the highest frequencies, which is an indication that the modes are localized.

E. Mean Free Paths

Using the lifetimes predicted from the structure factor peaks and the transverse sound speed, the MFP is about the size of the simulation cell L.

$$\Lambda_{AF}(\omega) = (3D_{AF,i}(\omega)\tau(\omega))^{1/2}, \qquad (27)$$

V. THERMAL CONDUCTIVITY

A. Bulk

BEGINALAN

To predict the bulk thermal conductivity for our models of a-SiO2 and a-Si, we use Eq. and the GK method.(cite) The GK method for predicting therma conductivity is relatively inexpensive compared to the NMD and AF methods so large system sizes can be studied (see Section). Similarly large systems were studied in Ref. 68. The details of the GK method are discussed in Section .

The GK-predicted thermal conductivity k_{GK} is plotted in Fig. for varying system sizes L. For a-SiO2, there is no apparent dependance of k_{GK} on L. For a-Si, there is

a clear dependance of k_{GK} on L. Assuming the DOS has the form of Eq. and the diffusivity scaling is quadratic (Eq.) for the low-frequncy modes in the system, the thermal conductivity as a function of the system size takes the form

$$\frac{k(L)}{k_{bulk}} = 1 - \frac{c_0}{L}, \tag{28}$$

where k_{bulk} is the extrapolated bulk thermal conductivity and c_0 is a constant. The extrapolation is performed using the three largest system sizes studied, including the tiled 800,000 atom sample (see Section). We do not observe that tiling a smaller a-Si model increases the thermal conductivity of a given system size above that predicted by Eq. , as was found in Ref 21. This is likely due to the small (512 atom) model used to perform the tiling. The success of Eq. for the dependance of k_{GK} on L for our model is in agreement with the qudratic scaling of the diffusivity for a-Si shown in Fig. and the Debye-scaling in Fig. .

To predict k_{vib} we choose ω_{cut}, the constant B for the diffusivity scaling, and the sound speed v_s. For both a-SiO2 and a-Si, we use the sound speeds predicted by a fit to the low-frequency DOS (Fig.).

For a-Si, the constant B for the quadratic scaling is chosen such that $D(\omega) = D_{AF,i}$ for $\omega_i = 1.16$ rad/s. This value of ω_{cut} is somewhat smaller than that used in Ref and . The constant B we find is somewhat larger than that found in Ref. and . We choose this ω because of the reasonable agreement between the AF-predicted D_{AF} and NMD-predicted D_{NMD} in this frequency region, shown in Fig. . We predict for a-Si $k_{ph} = 0.62$ W/m-K. Similar values for k_{ph} can be predicted by increasing ω_{cut} and decreasing B.

For a-Si a quadradic scaling is also considered using ω_{cut} from the study by . As there is no clear evidence of a quartic scaling of diffusivity, we choose the constant B which passes visibly through both D_{AF} and D_{NMD} in Fig. . When using the quartic diffusivity scaling $D(\omega) \propto \omega^{-4}$, the thermal conductivity is divergent as the frequency goes to zero. (cite) The thermal conductivity can be made finite using a boundary scattering models,(cite) such as the simple one considered in Section. While a fit to our model is not possible for the quartic scaling, it has been used to explain previous experimental measurements of a-Si thin films.(cite)

Baldi et al used a $\omega_{cut} = 4.55$ rads/s, which is a reasoable cut-off for our model of a-Si.[34] Baldi et al find that the contribution k_{ph} 0.1 W/m-K, which is the same as the contribution k_{ph} predicted in this work for a-SiO2. This contribution k_{ph} is smaller than the error bars in the predictions of k_{vib} and k_{GK} shown in Figs. and .

the quadractic scaling is responsible for the system size dependent thermal conductivity predicted by the GK method (k_{GK}, see Section) and seems to be the correct scaling to describe the low-frequency modes for our model of bulk a-Si. However,

Comparing with previous MD simulations of a-Si, Lee found a value of around 1 W/m-K but with very small supercell sizes.[107] He et al find for bulk a-Si $k_{vib} = 3$ W/m-K using the Tersoff potential and a linear extrapolation of the form Eq. using non-equillibrium molecular dynamics.

For smaller system sizes, the same trajectories are used for the GK and NMD methods. The MD simulations were run with the same parameters as the NMD metho (see Section).

The predicted thermal condcutivties from the GK method are plotted in Fig. . For a-SiO2, the thermal conductivity is size independent within the errors. For a-Si, there is a clear size-dependance of the thermal conductivity

To compare the results of the mode-based methods (NMD and AF) and the GK method, it is necessary to estimate the missing contribution from vibrational modes with frequency less than the minimum frequency of the finnite systems.

"We find that we cannot define a wave vector for the majority of the states, but the intrinsic harmonic diffusivity is still well-defined and has a numerical value similar to what one gets by using the Boltzmann result, replacing v by a sound velocity and replacing l by an interatomic distance a. "[19]

"In order to fit the experimental sc(T) it is necessary to add a Debye- like continuation from 10 meV down to 0 meV. The harmonic diffusivity becomes a Rayleigh m law and gives a divergent (T) as T O. To eliminate this we make the standard assumption of resonant- plus-relaxational absorption from two-level systems (this is an anharmonic effect which would lie outside our model even if it did contain two-level systems implicitly). "[19]

The same ω_{cut} was used by Cahill et al. together with a Rayleigh scaling and a boundary scattering model to find $k_{ph} = 0.31$ W/m-K.[28]

The relative contribution of k_{ph} and k_{AF} is also predicted to be similar for silicon nanowires.[70]

The comparison between theory and experi- ment supports the description of heat transport in disordered materials developed in Ref. 10, namely, that the dominant heat transport mech- anism is coupling between nearly degenerate, extended, but nonpropagating vibrational modes.

B. Accumulation Function

BEGIN$_A LAN$

The thermal conductivity accumulation function,

$$k(\Lambda_{cut}) = \frac{1}{V}\int_0^{\Lambda_{cut}} kbD(\Lambda)DOS(\Lambda) + \frac{1}{V}\sum_{\Lambda<\Lambda_{cut}} kbv_{AF}\Lambda_{AF}, \tag{29}$$

is predicted using our models of bulk a-SiO2 and a-Si and shown in Fig. . For the phonon contribution k_{ph}, the mode diffusivites ($D(\omega)$ can be transformed $D(\Lambda) =$

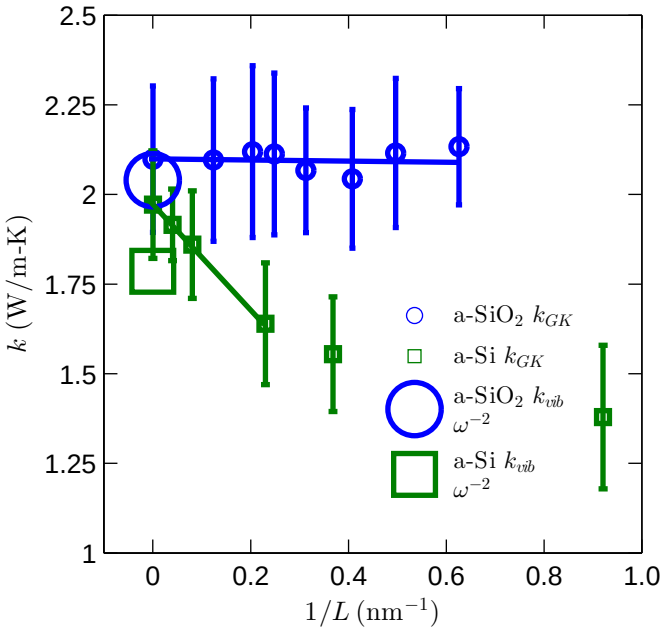

FIG. 6: Thermal conductivities of a-SiO^2*anda* – *Sipredicedusingthe GK method. For a* – *SiO2, thethermalconductivityissize* – *independent, indicatingthereisnoimportantcontributionfromphonons(Eq.(2)).Whilea* – *Si, thereisaclearsizedependance, whichisaccountedforbyusingEq.(8)ona-SiO2and a-Si* extrapolation (Eq. (7), Fig. 4).

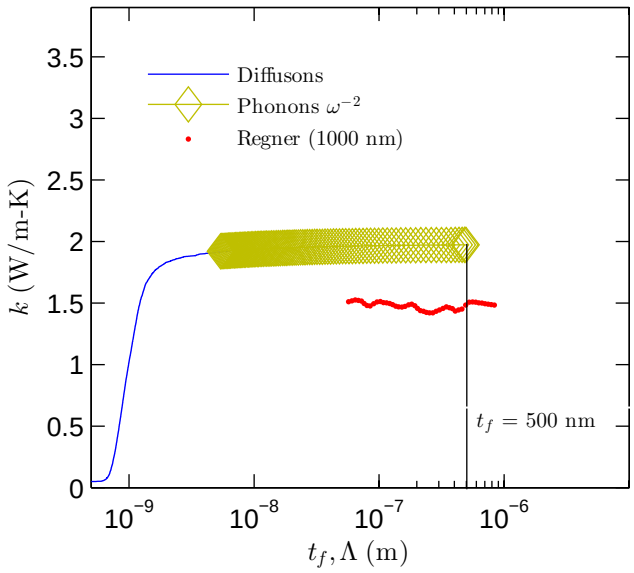

FIG. 7: Thermal conductivity accumulations and thermal conducitivities versus film thickness for a-SiO2 (top plot) and a-Si (bottom plot) from: (i) predictions from this work, (ii) recent broadband measurements of Regner et al, (iii) various experimental measurements for a wide-range of a-Si film thicknesses (Eq. (2)). While the thermal conductivity predictions for a-SiO2 and a-Si in this work seem to be well-characterized by Umklapp type scaling of the MFPs (Eq. (7)), this scaling is not able to predict the dramatic increase of thermal conducitivity with increasing film thickness from experimentl measurements of a-Si thin films.

$D(\omega)/v_s$. A simple boundary scattering based on the film thickness t_f and the Matthiesen rule is used,

The thermal conductivity accumulation functions for a-SiO2 and a-Si thin films are shown in Fig. . The thermal conductivity accumulation function for a-SiO2 saturates at a MFP of 10 nm, which is on the order of the finite size of our model (Section). This sharp accumulation at small MFPs is in good agreement with the prediction that k_{AF} is the dominant contribution to k_{vib}. This result is also in accord with the penetration depth-independent thermal concudcitivity measurements using broadband FDTR.[22] Only the quadratic scaling Eq. is considered for a-SiO2, which is discussed later in Section .

For a-Si, the thermal conductivity accumulation function shows that k_{AF} saturates before 10 nm, which is also on the order of our finite model size. The propagating contribution k_{ph} is predicted using both quadratic (Eq.) and quartic (Eq.) scaling for the mode diffusivities. As discussed in Section, the quadractic scaling is responsible for the system size dependent thermal conductivity predicted by the GK method (k_{GK}, see Section) and seems to be the correct scaling to describe the low-frequency modes for our model of bulk a-Si. Using the quadratic scaling, the thermal accumulation functions for our model of a-Si thin films passes reasonably well through many of the experimentally measured values.(cite) The quartic scaling also passes through many of the experimentally measured values reasonably well, particularly for film thicknesses larger than 10 μm.(cite)

END$_A LAN$

C. Discussion

BEGIN$_A LAN$

The transverse sound speed predicted for our model of a-Si is about 85% of that measured by experiment.[31] The same is true for a-SiO2. While this possibly leads to an underprediction of the mode diffusivitiy scalings we predict (Eq. , Fig.), it leads to an overprediction of the DOS (Eq.). Overall this leads to an underprediction of the thermal conductivity because the DOS scales as $DOS(\omega) \propto 1/v_s^3$. We can thus regard the predictions from our models, with smaller transverse sound speeds, as an upper bound on k_{ph} for a given diffusivity scaling $D(\omega) = B\omega^{-2}$. The critical parameter is the choice of ω_{cut}.(cite) We pick ω_{cut} and the low frequency scaling $D(\omega) = B\omega^{-2}$ based on their ability to describe the low-frequency beavhior of the vibrational modes in our finite-size models. The quadradic scaling $D(\omega) = B\omega^{-2}$ has

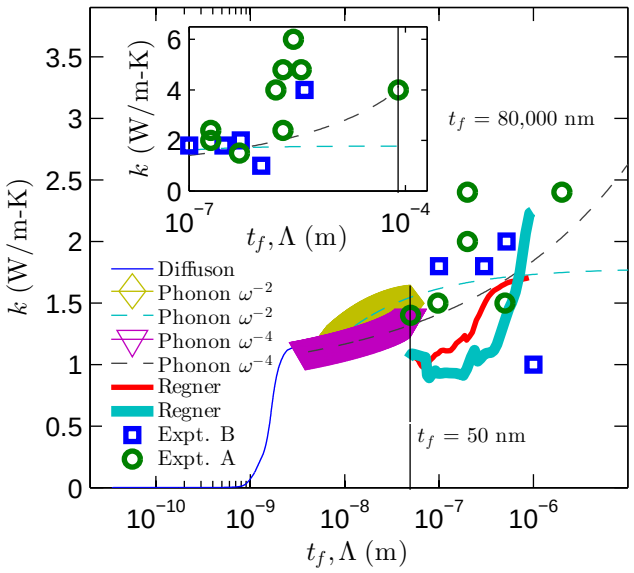

FIG. 8: film thickness dependant thermal conductivity of a-Si from experiment.

been observed in separate numerical studies for models of a-SiO2(cite) and a-Si(cite).

Previous experimental stduies of a-SiO2 have estimated negligible the contribution from low frequency ($\omega < \pi 10^1 2 rads/s$)[118] vibrational modes to be negligible. Using our model of a-SiO2, we also find the low-frequency propagating contribution to be negligible (Section). While experiments show there is are cross-over regions from quadratic to quartic scaling of the mode lifetimes in a-SiO2, the thermal conductivity of thin film a-SiO2 shows no significant dependance on the thickness.(cite) The cross-over region from quadratic to quartic, then back to quadratic observed in experiments for a-SiO2 occurs in the frequency range 4.610^9 to 1.5210^{10} rads/s,[39] and 3.0410^11 to 1.5210^{12} rads/s[41]. While these frequency ranges are inaccesible by our finite- size models, we estimate that the extraoplated k_{ph} using a quartic scaling in this region to be... The bulk thermal conductivity predicted for our model of a-SiO2 overstimates that of experimental measurements.[22] This can be attributed to either difference between experimental a-SiO2 and the potential model used in this work,(cite) the lack of anharmonic scattering included in the AF theory,[19] or the assumption of the classical-limit specfic heat for all frequencies (Section). Qualitatively, our model confirms that propagating modes do not contribute significantly to the thermal conductivity of a-SiO2.

The classical-limit mode specific heat is a good approximation for the low-frequency propagating modes in a-SiO2 and a-Si, which are shown to fully activated by around 10 K.(cite) The classic limit for the mode specific heat is an over-prediction for the high frequency modes in a-SiO2 and a-Si at 300 K.(cite) However, the contribution k_{AF} we predict in the classical limit for mode specific heat for a-Si is nearly the same as the the non-propagating contribution (plateau) predicted by broadband FTDR.(cite) Adjusting the specific heats to inclue quantum statstical effects... Taking the diffuson contribution k_{AF} to be a constant, which we predict to be $k_{AF} \approx 1$ W/m-K in agreement with other numerical studies(cite) and experiments(cite), we can thus focus on determing the less understood low-frequency propagating contribution k_{ph}.

There is a question as to the scaling of the low-frequenc vibrational mode lifetimes in a-Si. For a-SiO2, both quadractic and quartic scalings can be observed experimetnally.(cite) For a-Si thin films, varying preparation techniques suggest either quadratic(cite) or quartic(cite) scaling alone. While there is no clear consensus from various experiments, all predictions in this work demonstrate that the low-frequency modes in bulk a-Si follow a quadractic scaling of the mode lifetimes, which has been observed in previous models of a-Si(cite) and a-SiO2.(cite) Amorphous silicon, however, can be prepared only in thin films,(cite) where voids and other inho- mogeneities are unavoidable[117] and can influence the vibrational structure at low frequencies.[31,121] A smooth transition between quadratic and quartic scaling can be achieved using a phenomological model where a cross-over wavevector (or frequency) must be specified by experiment.[40] While this cross-over can be identified experimentally for a-SiO2,[39] experiments are limited for a-Si thin films.(cite) Our models are not large enough to investigate the relevevant frequency range ($< 110^{12}$ rads/s),(cite) so we considered both quadratic and quartic lifetime scalings when predicting the thermal conductivity accumulation functions in Fig. . Experimental measurements of the cross-over frequency (wavevector) and steepness parameter are needed from experiment to investigate the applicability of this phenomological model further.(cite) The dependance of a-Si thin film thermal conductivity on thickness,(cite) preparation method,(cite) and hydrogen content(cite) make this particularly challenging. In fact, different experimetnal studies can be satisfactorily explained using quadratic(cite) or quartic(cite) scalings found that each was a satisfactory explanation for the results found. (cite)

A number of emerging experimental techniques are capable of studying the low-frequency propagating modes in disordered systems. (cite) For amorphous materials, where the propagating contribution k_{ph} is typically smaller than in the crystalline phase, broadband FDTR has demonstrated it can probe the relatively small effect of propagating modes at 300 K. However, the broadband FDTR studies thus far have been limited to one deposition technique and a relatively small range of film thicknesses (500 nm $< t_f <$ 2000 nm).(cite) The nature of the low frequency scaling can be better elucidated using broadband FDTR on films prepared using varying

deposition techniques,(cite) a wider-range of film thicknesses (1-100 μm) (cite) and lower-range of temperatures ($10 - 100$ K).(cite) For a-Si, propagating low-frequency have been identified qualititatively by both exprimental measurements(cite) and numerical modeling.(cite) It is thus interetsing to consider thin films of a-SiGe alloys, which have been demonstrated to have reduced thermal conductivities compared to a-Si.[19] It is not clear what vibrational lifetime scaling at low frequency would be observed in a simple topologically disordered alloy given there isnt a consensus for even topologically disordered but chemically ordered systems.(cite) A combination of frequency-domain, time-domain, and variable-physical-heating size measurments would be helpful in investigating.[15,17,22,122]

END$_A LAN$

This supports the idea of Slack for a-SiO_2[115] While the thermal conductivity of a-SiO , the material is characterized by a constant similar for other amorphous materials such as Lennard-Jones argon[78] and a model of a-GeTe.[69]

That the amorphous phase of Si should have a lower GHz attenuation than many other amorphous materials is not entirely surprising, as the 2002 review of low-temperature thermal conductivity and internal friction by Pohl, Liu, and Thompson certainly indicates that the fourfold coordinated materials tend to demonstrate weaker anharmonicity.[90]

Theoretical predictions of acoustic attenuation in amor- phous solids generally agree that at room temperature, a quadratic frequency dependence is expected in the frequency range of 10 GHz1 THz and its origins are expected to be the anharmonicity of the interatomic bonds.

VI. SUMMARY

BEGIN$_A LAN$

In this work we investigated the contributions of propagating k_{ph} and non-propagatig k_{AF} modes to the total vibrational thermal conductivity k_{vib} of two glasses, a-SiO2 and a-Si. For a-SiO2, the contribution from propagating modes k_{ph} is shown to be negligible compared to k_{vib}. This is confirmed by various experimental measurements, including a broadband FDTR study which probed the vibrational MFPs or a-SiO2. The thermal conductivity accumulation function for our model of a-SiO2 saturates near a MFP of 10 nm, in agreement with the results of Regner et al. who show no systematic variation of the thermal conductivity on L_p,[22] and in agreement with experiments on a-SiO2 thin films which show no systematic variation with film thickness t_f.(cite)

Our model of bulk a-Si has a thermal conductivity k_{vib} with significant contribution from k_{ph}, where the low-frequency propagating modes are best described by a quadratic scaling of the mode lifetimes. The thermal conductivity accumulation predicted for our model of bulk a-Si with a simple boundary scattering model show resonable agreement with some of the experimentally predicted thermal conductivities using varying film thicknesses and deposition techniques (Fig.).(cite) However, using a quartic scaling with our model also gives a satisfactory agreement with other experimental measurements (Fig.).(cite) These large discrepancies between measured thermal conductivity of various a-Si thin films calls for the need of further experimentation. Broadband techniques,(cite) which have demonsrated the ability to probe a wide-range of vibrational mode frequencies and MFPs, can help elucidate.(cite)

END$_A LAN$

1. D. G. Cahill, W. K. Ford, K. E. Goodson, G. D. Mahan, A. Majumdar, H. J. Maris, R. Merlin, and S. R. Phillpot, Journal of Applied Physics **93**, 793818 (2003).
2. J.-K. Yu, S. Mitrovic, D. Tham, J. Varghese, and J. R. Heath, Nature Nanotechnology **5**, 718721 (2010).
3. A. I. Hochbaum, R. Chen, R. D. Delgado, W. Liang, E. C. Garnett, M. Najarian, A. Majumdar, and P. Yang, Nature **451**, 163167 (2008).
4. G. Pernot, M. Stoffel, I. Savic, F. Pezzoli, P. Chen, G. Savelli, A. Jacquot, J. Schumann, U. Denker, I. Mnch, et al., Nat Mater **9**, 491 (2010), ISSN 1476-1122, URL `http://dx.doi.org/10.1038/nmat2752`.
5. A. I. Boukai, Y. Bunimovich, J. Tahi-Kheli, J.-K. Yu, W. A. G. Goddard, and J. R. Heath, Nature **451**, 168171 (2008).
6. B. Poudel, Q. Hao, Y. Ma, Y. Lan, A. Minnich, B. Yu, X. Yan, D. Wang, A. Muto, D. Vashaee, et al., Science **320**, 634638 (2008), URL `http://www.sciencemag.org/content/320/5876/634.abstract`.
7. A. Ward and D. A. Broido, Phys. Rev. B **81**, 085205 (2010), URL `http://link.aps.org/doi/10.1103/PhysRevB.81.085205`.
8. M. G. Holland, Physical Review **132**, 2461 (1963).
9. J. J. Freeman and A. C. Anderson, Physical Review B **34**, 5684\textbackslashtextbackslashtextbackslash965690 (1986).
10. D. G. Cahill, S. K. Watson, and R. O. Pohl, Phys. Rev. B **46**, 61316140 (1992), URL `http://link.aps.org/doi/10.1103/PhysRevB.46.6131`.
11. R. J. von Gutfeld and A. H. Nethercot, Phys. Rev. Lett. **12**, 641644 (1964), URL `http://link.aps.org/doi/10.1103/PhysRevLett.12.641`.
12. G. D. Mahan and F. Claro, Phys. Rev. B **38**, 19631969 (1988), URL `http://link.aps.org/doi/10.1103/PhysRevB.38.1963`.
13. G. Chen, Journal of Nanoparticle Research **2**, 199 (2000), ISSN 1388-0764, URL `http://dx.doi.org/10.1023/A%3A1010003718481`.
14. A. D. Christianson, M. D. Lumsden, O. Delaire, M. B. Stone, D. L. Abernathy, M. A. McGuire, A. S. Sefat, R. Jin, B. C. Sales, D. Mandrus, et al., Phys. Rev. Lett. **101**, 157004 (2008), URL `http://link.aps.org/doi/10.1103/PhysRevLett.101.157004`.
15. Y. K. Koh and D. G. Cahill, Phys. Rev. B **76**, 075207 (2007), URL `http://link.aps.org/doi/10.1103/PhysRevB.76.075207`.
16. M. Highland, B. C. Gundrum, Y. K. Koh, R. S. Averback, D. G. Cahill, V. C. Elarde, J. J. Coleman, D. A. Walko, and E. C. Landahl, Phys. Rev. B **76**, 075337 (2007), URL `http://link.aps.org/doi/10.1103/PhysRevB.76.075337`.
17. A. J. Minnich, J. A. Johnson, A. J. Schmidt, K. Esfarjani, M. S. Dresselhaus, K. A. Nelson, and G. Chen, Phys. Rev. Lett. **107**, 095901 (2011), URL `http://link.aps.org/doi/10.1103/PhysRevLett.107.095901`.
18. F. Yang and C. Dames, Physical Review B **87**, 035437 (2013), URL `http://link.aps.org/doi/10.1103/PhysRevB.87.035437`.
19. J. L. Feldman, M. D. Kluge, P. B. Allen, and F. Wooten, Physical Review B **48**, 1258912602 (1993).
20. J. L. Feldman, P. B. Allen, and S. R. Bickham, Phys. Rev. B **59**, 35513559 (1999), URL `http://link.aps.org/doi/10.1103/PhysRevB.59.3551`.
21. Y. He, D. Donadio, J.-H. Lee, J. C. Grossman, and G. Galli, ACS Nano **5**, 1839\textbackslashtextbackslashtextbackslashtextbackslashtextbacksl (2011).
22. K. T. Regner, D. P. Sellan, Z. Su, C. H. Amon, A. J. McGaughey, and J. A. Malen, Nat Commun **4**, 1640 (2013), URL `http://dx.doi.org/10.1038/ncomms2630`.
23. S.-M. Lee and D. G. Cahill, Journal of Applied Physics **81**, 25902595 (1997).
24. T. Yamane, N. Nagai, S.-i. Katayama, and M. Todoki, Journal of Applied Physics **91**, 97729776 (2002), URL `http://link.aip.org/link/?JAP/91/9772/1`.
25. H. Wada and T. Kamijoh, Japanese Journal of Applied Physics **35**, L648L650 (1996), URL `http://jjap.jsap.jp/link?JJAP/35/L648/`.
26. B. L. Zink, R. Pietri, and F. Hellman, Physical Review Letters **96**, 055902 (2006), URL `http://link.aps.org/doi/10.1103/PhysRevLett.96.055902`.
27. H.-S. Yang, D. G. Cahill, X. Liu, J. L. Feldman, R. S. Crandall, B. A. Sperling, and J. R. Abelson, Phys. Rev. B **81**, 104203 (2010), URL `http://link.aps.org/doi/10.1103/PhysRevB.81.104203`.
28. D. G. Cahill, M. Katiyar, and J. R. Abelson, Physical Review B **50**, 60776081 (1994).
29. B. S. W. Kuo, J. C. M. Li, and A. W. Schmid, Applied Physics A: Materials Science & Processing **55**, 289296 (1992), ISSN 0947-8396, 10.1007/BF00348399, URL `http://dx.doi.org/10.1007/BF00348399`.
30. S. Moon, M. Hatano, M. Lee, and C. P. Grigoropoulos, International Journal of Heat and Mass Transfer **45**, 2439 2447 (2002), ISSN 0017-9310, URL `http://www.sciencedirect.com/science/article/pii/S0017931001003477`.
31. X. Liu, J. L. Feldman, D. G. Cahill, R. S. Crandall, N. Bernstein, D. M. Photiadis, M. J. Mehl, and D. A. Papaconstantopoulos, Phys. Rev. Lett. **102**, 035901 (2009), URL `http://link.aps.org/doi/10.1103/PhysRevLett.102.035901`.
32. L. Wieczorek, H. Goldsmid, and G. Paul, in *Thermal Conductivity 20*, edited by D. Hasselman and J. Thomas, J.R. (Springer US, 1989), pp. 235–241, ISBN 978-1-4612-8069-9, URL `http://dx.doi.org/10.1007/978-1-4613-0761-7_22`.
33. J. L. Feldman, Journal of Non-Crystalline Solids **307310**, 128 (2002), ISSN 0022-3093, URL `http://www.sciencedirect.com/science/article/pii/S0022309302014503`.
34. G. Baldi, V. M. Giordano, G. Monaco, F. Sette, E. Fabiani, A. Fontana, and G. Ruocco, Phys. Rev. B **77**, 214309 (2008), URL `http://link.aps.org/doi/10.1103/PhysRevB.77.214309`.
35. G. Baldi, V. M. Giordano, G. Monaco, and B. Ruta, Phys. Rev. Lett. **104**, 195501 (2010), URL `http://link.aps.org/doi/10.1103/PhysRevLett.104.195501`.
36. R. C. Zeller and R. O. Pohl, Phys. Rev. B **4**, 20292041 (1971), URL `http://link.aps.org/doi/10.1103/PhysRevB.4.2029`.
37. J. E. Graebner, B. Golding, and L. C. Allen, Phys. Rev. B **34**, 56965701 (1986), URL `http://link.aps.org/doi/`

10.1103/PhysRevB.34.5696.
[38] A. Wischnewski, U. Buchenau, A. J. Dianoux, W. A. Kamitakahara, and J. L. Zarestky, Phys. Rev. B **57**, 26632666 (1998), URL http://link.aps.org/doi/10.1103/PhysRevB.57.2663.
[39] C. Masciovecchio, G. Baldi, S. Caponi, L. Comez, S. Di Fonzo, D. Fioretto, A. Fontana, A. Gessini, S. C. Santucci, F. Sette, et al., Phys. Rev. Lett. **97**, 035501 (2006), URL http://link.aps.org/doi/10.1103/PhysRevLett.97.035501.
[40] G. Baldi, V. M. Giordano, and G. Monaco, Phys. Rev. B **83**, 174203 (2011), URL http://link.aps.org/doi/10.1103/PhysRevB.83.174203.
[41] G. Baldi, M. Zanatta, E. Gilioli, V. Milman, K. Refson, B. Wehinger, B. Winkler, A. Fontana, and G. Monaco, Phys. Rev. Lett. **110**, 185503 (2013), URL http://link.aps.org/doi/10.1103/PhysRevLett.110.185503.
[42] W. Schirmacher, EPL (Europhysics Letters) **73**, 892 (2006), URL http://stacks.iop.org/0295-5075/73/i=6/a=892.
[43] W. Schirmacher, G. Ruocco, and T. Scopigno, Phys. Rev. Lett. **98**, 025501 (2007), URL http://link.aps.org/doi/10.1103/PhysRevLett.98.025501.
[44] B. Schmid and W. Schirmacher, Phys. Rev. Lett. **100**, 137402 (2008), URL http://link.aps.org/doi/10.1103/PhysRevLett.100.137402.
[45] W. Schirmacher, B. Schmid, C. Tomaras, G. Viliani, G. Baldi, G. Ruocco, and T. Scopigno, physica status solidi (c) **5**, 862 (2008), ISSN 1610-1642, URL http://dx.doi.org/10.1002/pssc.200777584.
[46] C. Ganter and W. Schirmacher, Phys. Rev. B **82**, 094205 (2010), URL http://link.aps.org/doi/10.1103/PhysRevB.82.094205.
[47] B. Ruffl, M. Foret, E. Courtens, R. Vacher, and G. Monaco, Phys. Rev. Lett. **90**, 095502 (2003), URL http://link.aps.org/doi/10.1103/PhysRevLett.90.095502.
[48] M. Wyart, EPL (Europhysics Letters) **89**, 64001 (2010), URL http://stacks.iop.org/0295-5075/89/i=6/a=64001.
[49] S. N. Taraskin and S. R. Elliott, Phys. Rev. B **61**, 1201712030 (2000), URL http://link.aps.org/doi/10.1103/PhysRevB.61.12017.
[50] S. Ciliberti, T. S. Grigera, V. Martin-Mayor, G. Parisi, and P. Verrocchio, The Journal of Chemical Physics **119**, 8577 (2003), URL http://link.aip.org/link/?JCP/119/8577/1.
[51] G. Pompe and E. Hegenbarth, physica status solidi (b) **147**, 103 (1988), ISSN 1521-3951, URL http://dx.doi.org/10.1002/pssb.2221470109.
[52] D. G. Cahill, H. E. Fischer, T. Klitsner, E. T. Swartz, and R. O. Pohl, Journal of Vaccuum Science and Technology A **7**, 12591266 (1989).
[53] B. L. Zink, R. Islam, D. J. Smith, and F. Hellman, Phys. Rev. B **74**, 205209 (2006), URL http://link.aps.org/doi/10.1103/PhysRevB.74.205209.
[54] J. Fabian and P. B. Allen, Phys. Rev. Lett. **82**, 14781481 (1999), URL http://link.aps.org/doi/10.1103/PhysRevLett.82.1478.
[55] W. Gtze and M. R. Mayr, Phys. Rev. E **61**, 587606 (2000), URL http://link.aps.org/doi/10.1103/PhysRevE.61.587.
[56] H. Shintani and H. Tanaka, Nat Mater **7**, 870 (2008), ISSN 1476-1122, URL http://dx.doi.org/10.1038/nmat2293.
[57] J. Horbach, W. Kob, and K. Binder, The European Physical Journal B - Condensed Matter and Complex Systems **19**, 531 (2001), ISSN 1434-6028, URL http://dx.doi.org/10.1007/s100510170299.
[58] G. Ruocco and F. Sette, Journal of Physics: Condensed Matter **13**, 9141 (2001), URL http://stacks.iop.org/0953-8984/13/i=41/a=307.
[59] P. Benassi, M. Krisch, C. Masciovecchio, V. Mazzacurati, G. Monaco, G. Ruocco, F. Sette, and R. Verbeni, Phys. Rev. Lett. **77**, 38353838 (1996), URL http://link.aps.org/doi/10.1103/PhysRevLett.77.3835.
[60] J. K. Christie, S. N. Taraskin, and S. R. Elliott, Journal of Non-Crystalline Solids **353**, 2272 (2007), ISSN 0022-3093, URL http://www.sciencedirect.com/science/article/pii/S0022309307002840.
[61] W. Schirmacher, G. Diezemann, and C. Ganter, Phys. Rev. Lett. **81**, 136139 (1998), URL http://link.aps.org/doi/10.1103/PhysRevLett.81.136.
[62] S. N. Taraskin, Y. L. Loh, G. Natarajan, and S. R. Elliott, Phys. Rev. Lett. **86**, 12551258 (2001), URL http://link.aps.org/doi/10.1103/PhysRevLett.86.1255.
[63] V. Martin-Mayor, M. Mezard, G. Parisi, and P. Verrocchio, The Journal of Chemical Physics **114**, 8068 (2001), URL http://link.aip.org/link/?JCP/114/8068/1.
[64] T. Scopigno, M. D'astuto, M. Krisch, G. Ruocco, and F. Sette, Phys. Rev. B **64**, 012301 (2001), URL http://link.aps.org/doi/10.1103/PhysRevB.64.012301.
[65] N. W. Ashcroft and N. D. Mermin, *Solid State Physics* (Saunders, Fort Worth, 1976).
[66] M. T. Dove, *Introduction to Lattice Dynamics* (Cambridge, Cambridge, 1993).
[67] J. M. Ziman, *Electrons and Phonons* (Oxford, New York, 2001).
[68] Y. He, D. Donadio, and G. Galli, Applied Physics Letters **98**, 144101 (2011), URL http://link.aip.org/link/?APL/98/144101/1.
[69] G. C. Sosso, D. Donadio, S. Caravati, J. Behler, and M. Bernasconi, Phys. Rev. B **86**, 104301 (2012), URL http://link.aps.org/doi/10.1103/PhysRevB.86.104301.
[70] D. Donadio and G. Galli, Phys. Rev. Lett. **102**, 195901 (2009).
[71] A. J. H. McGaughey and M. Kaviany, International Journal of Heat and Mass Transfer **47**, 17831798 (2004).
[72] D. A. McQuarrie, *Statistical Mechanics* (University Science Books, Sausalito, 2000).
[73] A. J. H. McGaughey and M. Kaviany, Physical Review B **69**, 094303 (2004).
[74] J. V. Goicochea, M. Madrid, and C. H. Amon, Journal of Heat Transfer **132**, 012401 (2010).
[75] P. B. Allen and J. L. Feldman, Physical Review B **48**, 1258112588 (1993).
[76] P. B. Allen and J. Kelner, American Journal of Physics **66**, 497506 (1998).
[77] D. Cahill and R. Pohl, Annual Review of Physical Chemistry **39**, 93121 (1988).
[78] J. Larkin and A. McGaughey, Journal of Applied Physics (2013).
[79] G. T. Barkema and N. Mousseau, Phys. Rev. B **62**, 49854990 (2000), URL http://link.aps.org/doi/10.1103/PhysRevB.62.4985.
[80] M. Durandurdu and D. A. Drabold, Phys. Rev. B **66**, 155205 (2002), URL http://link.aps.org/doi/10.

1103/PhysRevB.66.155205.
[81] N. Bernstein, J. L. Feldman, and M. Fornari, Phys. Rev. B **74**, 205202 (2006), URL http://link.aps.org/doi/10.1103/PhysRevB.74.205202.
[82] S. Plimpton, Journal of Computational Physics **117**, 1 19 (1995), ISSN 0021-9991, URL http://www.sciencedirect.com/science/article/pii/S002199918571039X.
[83] J. D. Gale and A. L. Rohl, Molecular Simulation **29**, 291 (2003).
[84] M. L. Williams and H. J. Maris, Phys. Rev. B **31**, 45084515 (1985), URL http://link.aps.org/doi/10.1103/PhysRevB.31.4508.
[85] Y. M. Beltukov, V. I. Kozub, and D. A. Parshin, Phys. Rev. B **87**, 134203 (2013), URL http://link.aps.org/doi/10.1103/PhysRevB.87.134203.
[86] S. N. Taraskin and S. R. Elliott, EPL (Europhysics Letters) **39**, 37 (1997), URL http://stacks.iop.org/0295-5075/39/i=1/a=037.
[87] V. Vitelli, N. Xu, M. Wyart, A. J. Liu, and S. R. Nagel, Phys. Rev. E **81**, 021301 (2010), URL http://link.aps.org/doi/10.1103/PhysRevE.81.021301.
[88] T. Hori, T. Shiga, and J. Shiomi, Journal of Applied Physics **113**, 203514 (2013), URL http://link.aip.org/link/?JAP/113/203514/1.
[89] J. C. Duda, T. S. English, D. A. Jordan, P. M. Norris, and W. A. Soffa, Journal of Physics: Condensed Matter **23**, 205401 (2011), URL http://stacks.iop.org/0953-8984/23/i=20/a=205401.
[90] R. O. Pohl, X. Liu, and E. Thompson, Rev. Mod. Phys. **74**, 9911013 (2002), URL http://link.aps.org/doi/10.1103/RevModPhys.74.991.
[91] W. Senn, G. Winterling, M. Grimsditch, and M. Brodsky, in *Inst. Phys. Conf. Ser* (1979), p. 709.
[92] R. Vacher, H. Sussner, and M. Schmidt, Solid State Communications **34**, 279 (1980), ISSN 0038-1098, URL http://www.sciencedirect.com/science/article/pii/0038109880905578.
[93] J. L. Feldman, J. Q. Broughton, and F. Wooten, Phys. Rev. B **43**, 21522158 (1991), URL http://link.aps.org/doi/10.1103/PhysRevB.43.2152.
[94] P. B. Allen, J. L. Feldman, J. Fabian, and F. Wooten, Philosophical Magazine B **79**, 17151731 (1999).
[95] S. Volz and G. Chen, Physical Review B **61**, 26512656 (2000).
[96] N. L. Green, D. Kaya, C. E. Maloney, and M. F. Islam, Physical Review E **83**, 051404 (2011), URL http://link.aps.org/doi/10.1103/PhysRevE.83.051404.
[97] R. Biswas, A. M. Bouchard, W. A. Kamitakahara, G. S. Grest, and C. M. Soukoulis, Phys. Rev. Lett. **60**, 22802283 (1988), URL http://link.aps.org/doi/10.1103/PhysRevLett.60.2280.
[98] L. E. Silbert, A. J. Liu, and S. R. Nagel, Phys. Rev. E **79**, 021308 (2009), URL http://link.aps.org/doi/10.1103/PhysRevE.79.021308.
[99] B. Ruzicka, T. Scopigno, S. Caponi, A. Fontana, O. Pilla, P. Giura, G. Monaco, E. Pontecorvo, G. Ruocco, and F. Sette, Phys. Rev. B **69**, 100201 (2004), URL http://link.aps.org/doi/10.1103/PhysRevB.69.100201.
[100] J. Fabian and P. B. Allen, Phys. Rev. Lett. **77**, 38393842 (1996), URL http://link.aps.org/doi/10.1103/PhysRevLett.77.3839.
[101] S. R. Bickham and J. L. Feldman, Phys. Rev. B **57**, 1223412238 (1998), URL http://link.aps.org/doi/10.1103/PhysRevB.57.12234.
[102] S. R. Bickham, Phys. Rev. B **59**, 48944897 (1999), URL http://link.aps.org/doi/10.1103/PhysRevB.59.4894.
[103] S. N. Taraskin and S. R. Elliott, Philosophical Magazine Part B **79**, 17471754 (1999), URL http://www.tandfonline.com/doi/abs/10.1080/13642819908223057.
[104] A. J. C. Ladd, B. Moran, and W. G. Hoover, Physical Review B **34**, 50585064 (1986).
[105] J. E. Turney, E. S. Landry, A. J. H. McGaughey, and C. H. Amon, Phys. Rev. B **79**, 064301 (2009), URL http://link.aps.org/doi/10.1103/PhysRevB.79.064301.
[106] J. M. Larkin, J. E. Turney, A. D. Massicotte, C. H. Amon, and A. J. H. McGaughey, to appear in Journal of Computational and Theoretical Nanoscience (2012).
[107] Y. H. Lee, R. Biswas, C. M. Soukoulis, C. Z. Wang, C. T. Chan, and K. M. Ho, Phys. Rev. B **43**, 65736580 (1991), URL http://link.aps.org/doi/10.1103/PhysRevB.43.6573.
[108] V. Mazzacurati, G. Ruocco, and M. Sampoli, EPL (Europhysics Letters) **34**, 681 (1996), URL http://stacks.iop.org/0295-5075/34/i=9/a=681.
[109] J. Fabian, J. L. Feldman, C. S. Hellberg, and S. M. Nakhmanson, Phys. Rev. B **67**, 224302 (2003), URL http://link.aps.org/doi/10.1103/PhysRevB.67.224302.
[110] P. Sheng and M. Zhou, Science **253**, 539542 (1991), URL http://www.sciencemag.org/content/253/5019/539.abstract.
[111] J. T. Edwards and D. J. Thouless, Journal of Physics C: Solid State Physics **5**, 807 (1972), URL http://stacks.iop.org/0022-3719/5/i=8/a=007.
[112] W. Garber, F. M. Tangerman, P. B. Allen, and J. L. Feldman, Philosophical Magazine Letters **81**, 433439 (2001), URL http://www.tandfonline.com/doi/abs/10.1080/09500830110041666.
[113] N. Xu, V. Vitelli, M. Wyart, A. J. Liu, and S. R. Nagel, Phys. Rev. Lett. **102**, 038001 (2009), URL http://link.aps.org/doi/10.1103/PhysRevLett.102.038001.
[114] C. Kittel, Physical Review **75**, 974 (1949).
[115] G. A. Slack (Academic Press, 1979), vol. 34 of *Solid State Physics*, p. 1 71, URL http://www.sciencedirect.com/science/article/pii/S0081194708603598.
[116] G. Ruocco, F. Sette, R. Di Leonardo, G. Monaco, M. Sampoli, T. Scopigno, and G. Viliani, Phys. Rev. Lett. **84**, 57885791 (2000), URL http://link.aps.org/doi/10.1103/PhysRevLett.84.5788.
[117] S. Li, Y. Jiang, Z. Wu, J. Wu, Z. Ying, Z. Wang, W. Li, and G. J. Salamo, Applied Surface Science **257**, 8326 (2011), ISSN 0169-4332, URL http://www.sciencedirect.com/science/article/pii/S0169433211004715.
[118] M. S. Love and A. C. Anderson, Phys. Rev. B **42**, 18451847 (1990), URL http://link.aps.org/doi/10.1103/PhysRevB.42.1845.
[119] A. M. Bouchard, R. Biswas, W. A. Kamitakahara, G. S. Grest, and C. M. Soukoulis, Phys. Rev. B **38**, 1049910506 (1988), URL http://link.aps.org/doi/10.1103/PhysRevB.38.10499.
[120] P. G. Klemens, Proceedings of the Physical Society. Section A **68** (1955).
[121] J. L. Feldman, N. Bernstein, D. A. Papaconstantopoulos, and M. J. Mehl, Phys. Rev. B **70**, 165201 (2004), URL http://link.aps.org/doi/10.1103/PhysRevB.70.

165201.
[122] M. E. Siemens, Q. Li, R. Yang, K. A. Nelson, E. H. Anderson, M. M. Murnane, and H. C. Kapteyn, Nature Materials **9**, 2630 (2010).